Charles University in Prague

Faculty of Science

Biology

Department of Experimental Plant Biology

Václav Svoboda

Role of PsbO isoforms in *Arabidopsis thaliana*

Master thesis

Role izoforem PsbO v *Arabidopsis thaliana*

Diplomová práce

Prague, 2016

Supervisor:

Mgr. Miloš Duchoslav

Advisor:

RNDr. Lukáš Fischer, Ph.D.

Statement:

I hereby state that I have completed this thesis by myself, and that I have properly cited all literature and other information sources I have used. Neither this thesis nor its parts have been submitted to achieve same or any other academic title.

Prohlášení:

Prohlašuji, že jsem závěrečnou práci zpracoval samostatně a že jsem uvedl všechny použité informační zdroje a literaturu. Tato práce ani její podstatná část nebyla předložena k získání jiného nebo stejného akademického titulu.

In Prague / v Praze 15.8.2016 Václav Svoboda

Acknowledgments

I would like to thank all the people that have helped with this thesis with their guidance and remarks. My biggest thanks go to my thesis supervisor Miloš Duchoslav for his patience, insightful advice and help with data evaluation. Inspiring thoughts suggested by the thesis advisor, Lukáš Fischer were especially helpful in the process of writing this thesis. I would also like to appreciate the friendly working environment shared by the colleagues in our laboratory.

Special thanks go to laboratory headed by Helena Lipavská for measurements of nonstructural saccharides. Thank you for giving me something more to think about.

On this place I would also like to thank Helmut Kirchhoff not only for the opportunity to work in his lab but especially for hosting me during my internship in Pullman. Work done in Helmut's lab has been integral for this thesis. For introducing me into biochemical techniques, sharing his knowledge and being good friend my thanks go to Sujith Puthiyaveetil.

I cannot forget to mentioned my friends Markéta and Jaroslav for their timely help with revision of the thesis. Many thanks to my friends and family that have been helpful not only during writing of this thesis but also throughout the course of my studies.

The thesis was elaborated with financial support of Charles University Grant Agency, project number 1472314 and by Ministry of Education, Youth and Sports of Czech Republic (project No. LO1417).

Role of PsbO isoforms in *Arabidopsis thaliana*

Abstract

Photosystem II (PSII) uses sunlight to catalyze water oxidation and reduce plastoquinone. Water oxidation takes place in oxygen evolving complex (OEC). OEC is stabilized by extrinsic subunits of PSII. The largest and most important of them is PsbO, manganese-stabilizing protein which can be found in all known oxygenic photosynthetic organisms. Model plant *Arabidopsis thaliana* expresses two isoforms of *psbO* gene, namely PsbO1and PsbO2.Mutants *psbo1* and *psbo2* lacking PsbO1 and PsbO2, respectively, recently brought new findings on the particular roles of isoforms in maintaining photosynthesis. PsbO1 is commonly considered as the main isoform facilitating water splitting, whereas PsbO2 is believed to be involved in PSII repair process (replacement of photodamaged D1 subunit).

This work focuses on particular roles of *Arabidopsis* PsbO isoforms in maintaining photosynthesis with special focus on response to light stress. Mutants *psbo1*, *psbo2* and wild type plants Col-0 were used for extensive biochemical investigation. Our aim was to find out what is the impact on overall thylakoid structure and composition in mutants. Furthermore, to investigate response to light stress in wild type regarding to yields of particular subcompartments, changes in photosystem II subpopulations and particularly, changes in distribution of PsbO isoforms.

We found that PsbO isoforms are distributed heterogeneously among thylakoid subcompartments (grana core, grana margins and stroma lamellae). PsbO2 showed more pronounced response to light stress than PsbO1, these findings support earlier hypothesis about role of PsbO2 in PSII repair cycle. We also found that PsbO accumulates in high amounts in lumen after exposure to light stress. Interestingly, our investigation regarding to *psbo1* mutant, lacking PsbO1 isoform, showed considerably impaired saccharide metabolism.

Key words

PsbO, manganese-stabilizing protein, photosystem II, digitonin fractionation, thylakoid subcomparments, lumen, light stress, nonstructural saccharides.

Role izoforem PsbO v *Arabidopsis thaliana*

Abstrakt

Fotosystém II (PSII) využívá sluneční energii k oxidaci vody a redukci plastochinonu. Oxidace vody probíhá na kyslík vyvíjejícím komplexu (OEC). OEC je stabilizován vnějšími podjednotkami PSII z nichž největší a nejdůležitější je PsbO, mangan-stabilizující protein, který se vyskytuje ve všech dosud známých oxygenních fotosyntetických organizmech. Modelová rostlina *Arabidopsis thaliana* exprimuje dvě izoformy genu *psbO*, jmenovitě PsbO1 a PsbO2. Nedávná pozorování mutantů *psbo1* a *psbo2*, kteří postrádají funkční geny *psbO1*, respektive *psbO2*, přinesla nové skutečnosti o konkrétních rolích izoforem PsbO při fotosyntéze. PsbO1 je obecně považována za hlavní izoformu umožňující efektivní rozklad vody, zatímco pro PsbO2 byla navržena role v opravných procesech PSII (výměna světlem poškozeného proteinu D1).

Tato práce je zaměřena na konkrétní role izoforem PsbO v *Arabidopsis* při fotosyntéze a zejména se soustředí na odpověď na světelný stres. Pro rozsáhlou biochemickou studii byli použiti mutanti *psbo1, psbo2* a wild type Col-0. Naším cílem bylo zjistit jak je ovlivněna celková struktura a složení thylakoidů u mutantů. Dále zjistit jak probíhá odpověď na světelný stres u wild type s ohledem na změny v množství jednotlivých subkompartmentů, změny v subpopulacích fotosystému II a zvláště pak na změny v distribuci izoforem PsbO.

Naše výsledky ukazují, že izoformy jsou v rámci subkompartmentů thylakoidní membrány (jader gran, okrajů gran a stromatálních lamel) distribuovány heterogenně. Izoforma PsbO2 vykazuje výraznější odpověď na světelný stres než izoforma PsbO1. Toto pozorování podporuje dřívější hypotézu, že PsbO2 se podílí na opravách poškozeného PSII. Po vystavení rostlin světelnému stresu jsme také pozorovali akumulaci vysokého množství PsbO v lumen thylakoidů. Zajímavá zjištění týkající se mutanta *psbo1* ukázala, že tento mutant, postrádající PsbO1, má značně narušený metabolismus sacharidů.

Klíčová slova

PsbO, mangan-stabilizující protein, fotosystém II, frakcionace digitoninem, thylakoidní subkompartmenty, lumen, světelný stres, nestrukturní sacharidy

Content

List of abbreviations

AA	acrylamide
APS	ammonium persulfate
BN-PAGE	blue-native polyacrylamide gel electrophoresis
BSA	bovine serum albumin
Car	carotenoids
Chl	chlorophyll
CURT	curvature thylakoid protein
cyt b_{559}	cytochrome b_{559}
cyt b_6f	cytochrome b_6f complex
D1	D1 protein, core subunit of photosystem II
DA	dark adapted
DW	dry weight
Fd	ferredoxin
FNR	ferredoxin-$NADP^+$ reductase
FW	fresh weight
GC	grana core
GL	growth light
GM	grana margins
GOE	great oxygenation event
GWD	genome wide duplication
HL	high light
HPLC	high-performance liquid chromatography
LHC	light harvesting complex
MC	megacomplexes
NPQ	non-photochemical quenching
NSS	nonstructural saccharides

OEC	oxygen evolving center
PBCP	photosystem II core phosphatase
PC	plastocyanin
PCR	polymerase chain reaction
PQ	plastoquinon
PQH2	plastoquinol, reduced form of plastoquinon
psbO1	gene coding PsbO1 protein
psbo1	plants lacking functional gene for PsbO1 protein
PsbO1	PsbO1 protein
psbO2	gene coding PsbO2 protein
psbo2	plants lacking functional gene for PsbO2 protein
PsbO2	PsbO2 protein
PSI	photosystem I
PSII	photosystem II
RC	reaction center of photosystem II
RT	room temperature
S.B.	sample buffer
SC	supercomplex of photosystem II
SDS	sodium dodecyl sulfate
SDS-PAGE	sodium dodecyl sulfate polyacrylamide gel electrophoresis
SL	stroma lamellae
TEMED	N,N,N',N'-tetramethylethylenediamine
VDE	violaxanthin de-epoxidase
WB	western blot
WR	working reagent
wt	wildtype

1 Introduction

Photosynthetic conversion of sunlight energy into chemical energy is undoubtedly the most important biological process on Earth. Sunlight energy is used to split water molecule into protons, electrons and oxygen. Protons and electrons are used to synthetize organic compounds and oxygen is released as a byproduct. Organisms capable to carry out oxygen photosynthesis such as plants, algae and cyanobacteria provide energy and nutrients. These so called primary producers stand in the beginning of the trophic chain, therefore directly or indirectly fuel almost all life (Hohmann-Marriott and Blankenship, 2011).

Prokaryotic cyanobacteria, first organisms able to perform oxygenic photosynthesis are believed to evolve more than 2.5 billion years ago. For a long period of time, cyanobacteria were the only primary producers and considerably changed our planet. First oxygen they produced was rapidly reduced by minerals and all oxide-minerals were created. After that, oxygen accumulated in planet atmosphere in process called Great Oxygenation Event (GOE). GOE drove evolution of eukaryotic cells and aerobic respiration. Photosynthetic cyanobacterium was subsequently domesticated by early eukaryote in event called primary endosymbiosis. It is believed that all primary plastids are derived from single event (McFadden and Van Dooren, 2004). These early algae evolved in diverse groups of photosynthetic eukaryotes crowned by higher plants (Hohmann-Marriott and Blankenship, 2011).

Photosynthesis begins on photosystem II, protein complex which uses sunlight energy for water oxidation in manganese cluster – oxygen evolving complex (OEC). Efficient water oxidation is facilitated by PsbO protein (manganese-stabilizing protein) which plays indispensable role in stabilization of OEC. Fundamental role of PsbO in photosynthesis can be demonstrated by its presence among all known oxygenic photosynthetic organisms (Roose et al., 2016). Recently, new findings turned out that *psbO* gene is in many angiosperms present in two copies. *Arabidopsis thaliana* is among the plants which expresses two copies of *psbO* gene, namely isoforms PsbO1 and PsbO2 (Duchoslav and Fischer, 2015).

This work focuses on *Arabidopsis* isoforms and their particular roles in maintaining photosynthesis. Mutants in either of the genes and wild type plants were used for this study. Special

focus is aimed to response of short light stress regarding to PsbO isoforms since plants have to constantly cope with light induced damage.

1.1 Aims of the Thesis

1) Comparison of *psbo1* and *psbo2* mutants regarding to thylakoid structure
2) Find out what is the distribution of PsbO isoforms among thylakoids subcompartments and how the distribution changes after exposure to light stress

2 Literature review

2.1 Thylakoids in higher plants

Thylakoid membrane, complex and highly specialized structure found in cyanobacterial cells and eukaryotic chloroplasts, is the site where light driven photosynthetic reactions take place.

Chloroplast and all of the other plastids are organelles of prokaryotic origin. Event when heterotrophic eukaryote domesticated photoautotrophic cyanobacteria is called primary endosymbiosis. To this day it is believed that all primary plastids are derived from a single event, which happened more than 600 million years ago, therefore plastids in photosynthetic eukaryotes have common ancestor (McFadden and Van Dooren, 2004).

Higher plant chloroplasts are semiautonomous, double membrane surrounded organelles found in so called "photosynthetic cells". Aqueous space within the inner membrane, where chloroplast DNA, ribosomes, numerous proteins, ions, nucleotides and all enzymes providing Calvin cycle reactions are found, is called stroma. In stroma is located specialized continuous thylakoid membrane system which encloses thylakoid lumen (Strittmatter et al., 2010).

Although photosynthetic reactions taking place in chloroplast stroma and thylakoids (TH) are inseparable, special attention will be devoted to thylakoids.

2.1.1 Thylakoid function

Photosynthesis is undoubtedly the most important biological process on Earth which directly or indirectly drives almost all life. The very unique feature of photosynthesis is its capability to convert sunlight (i.e. energy of photons) to chemical energy. Primary steps of this conversion take place on thylakoid membrane system which incorporate machinery of protein complexes (Fig. 1) needed for maintaining light driven reactions of photosynthesis (Rast et al., 2015).

Thylakoid function is therefore to carry out photosynthetic reactions starting with harvesting of sunlight (i.e. photons) by light harvesting complexes (LHC), protein complexes containing chlorophyll (Chl) and carotenoid (Car) molecules. Trapped photon is transferred by Förster resonance energy transfer to pigment-protein complex called photosystem II (PSII), particularly its reaction center (RC) where electron is excited to higher energy state and charge separation occurs. Electron missing in RC is immediately replenished by electron from water molecule oxidized in oxygen evolving center (OEC). Beside electrons also protons and oxygen as a byproduct are generated. Protons released into lumen help to increase proton gradient. Separated electrons are then used to reduce electron acceptor plastoquinone (PQ) to plastoquinole (PQH_2) which migrate throughout the thylakoid membrane bilayer towards cytochrome b_6f complex (Cyt b_6f). Cyt b_6f role is (i) creating of proton gradient through Q cycle which transfer protons into luminal space (ii) transfer of electrons from plastoquinole to plastocyanin (PC), another mobile electron carrier in thylakoids. Reduced PC migrates throughout the thylakoid lumen towards second pigment protein complex called photosystem I (PSI) where PC is oxidized by light excited state of PSI reaction center. PSI transfers electron to the last acceptor, water soluble ferredoxin (Fd), which becomes reduced and Fd transfer the electron to ferredoxin-$NADP^+$ reductase (FNR), enzyme capable to reduce $NADP^+$ to NADPH.

Proton gradient generated by water oxidation in OEC and by Cyt b_6f creates proton motive force driving chloroplast ATP synthase which create ATP in process called photophosphorylation. NADPH and ATP are subsequently used for carbon fixation (reviewed in Barber, 2012).

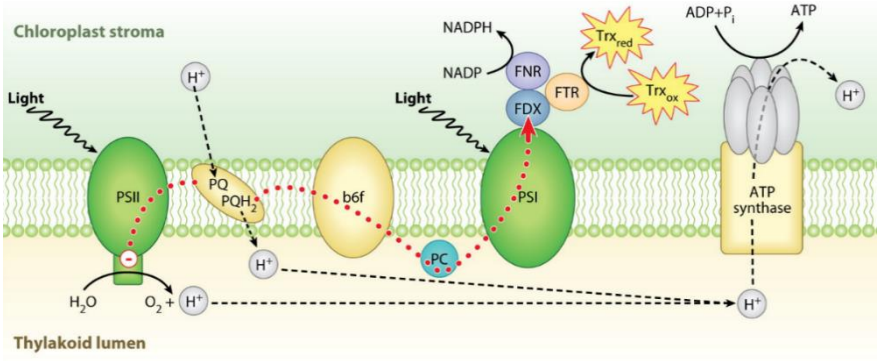

Figure 1. Light driven photosynthetic reaction on thylakoid membrane. Red dots represent route of electrons mediated by PQ/PQH_2 and PC. Dashed lines represent route of proton towards ATP synthase, where ATP is generated. (modified from Meyer et al., 2009)

Processes described above occur during well balanced environmental conditions that only rarely occur in the nature. Instead, sessile organism such a plant has to cope with ever changing environment and imbalanced energy input. Plants developed many ways how to avoid over-excitation in high light (HL) or how to harvest enough energy under low light conditions. As a result, thylakoids are highly dynamic structures with architectural and functional switches in the photosynthetic machinery.

2.1.2 Thylakoid structure

Land plant thylakoids have typical structure consisting of grana stack – appressed, cylindrical regions interconnected by stroma lamellae. Grana stacks consist of central grana core and peripheral grana margins (Fig. 2). Cylindrical grana stacks contain several membrane discs typically comprising of 10–20 layers of thylakoid membrane (Mustárdy and Garab, 2003) but in extreme cases it could be up to a hundred of layers as was reported for *Alocasia*, plant species living in shade of the tropical rainforest (Goodchild, D.J., Björkman, O., Pyliotis, 1972). Diameter of grana is typically in range 300–600 nm (Kirchhoff et al., 2011; Mustárdy and Garab, 2003), along with interconnecting unstacked stroma lamellae, grana stacks represent continuous thylakoid membrane system which encloses continuous thylakoids lumen (reviewed in Pribil et al., 2014).

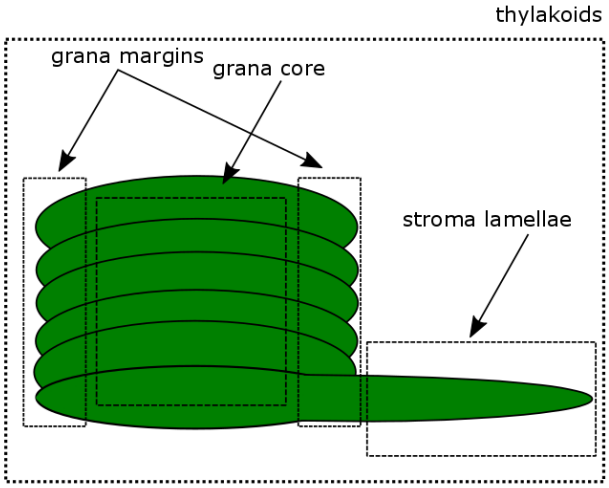

Figure 2. Higher plant thylakoid membrane architecture. Scheme is simplified, normally stroma lamellae is connected to another granum.

2.1.3 Lateral heterogeneity of thylakoid subcompartments

A closer look into the thylakoid structure reveals another typical characteristic of higher plant thylakoids, its lateral heterogeneity (Fig. 3), which points to the different protein complex composition in distinct thylakoid membrane subcompartments (Andersson and Anderson, 1980; Dekker and Boekema, 2005; Puthiyaveetil et al., 2014).

Thylakoid membrane can be divided into three membrane subcomparments: grana core (GC) host most PSII and its LHCII antennae in their densely stacked regions (Andersson and Anderson, 1980), grana margins (GM) with its curved shape due to high amounts of recently discovered curvature thylakoid (CURT) proteins (Armbruster et al., 2013) and stroma lamellae (SL), non-appressed grana interconnecting regions. PSI and ATPase are located in unstacked regions of SL, GM and grana end membranes – top and bottom of grana stacks (Albertsson, 2001). Cyt b_6f is assumed to be homogenously distributed in thylakoid membrane (Dekker and Boekema, 2005).

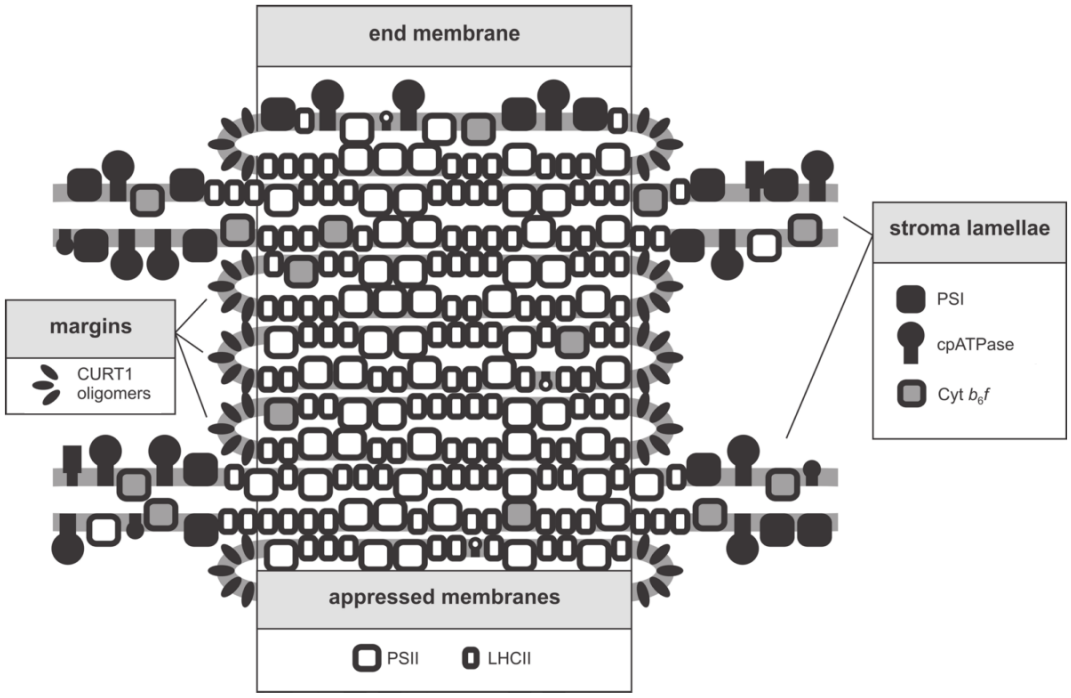

Figure 3. Lateral heterogeneity of thylakoid membrane of higher plants. Model is derived from electron microscopic images. Scheme do not show photosystem I (PSI) and ATPase in the grana margins (GM) regions. Cyt *b*6*f* in the grana can be significantly higher than shown in this scheme. (modified from Pribil et al., 2014)

PSII and LHCII localization in stacked grana is not accidental. Their flat stroma exposed surfaces (Nield and Barber, 2006; Wei et al., 2016) allow them to be accommodated in tightly appressed grana regions. On the other hand, PSI and ATPase with their bulky stroma protruding shape are excluded from grana stack because of steric hindrance (Ben-Shem et al., 2003; Junge et al., 2009). Clearly, different functions of listed subcompartments are dependent on lateral heterogeneity.

To obtain and study distinct subcompartments, intact thylakoids can be fractionated by mechanical treatments such as sonication (Wollenberger et al., 1995) or chemically by detergent. Digitonin proved to be the mildest option in detergent based fractionation treatments followed by ultracentrifugation which allow to obtain GC and SL (Cuello and Quiles, 2004). Puthiyaveetil et al. (2014) demonstrated even more advanced digitonin fractionation and obtained not only GC and SL but also GM fraction.

Although light is an essential factor for plant life and development, changes in irradiation rapidly changes during the day or season and causes stress. Coping with fluctuations in light intensity and quality is a basic prerequisite for plant survival. Over excitation during HL periods is the cause of light induced damage of photosynthetic machinery – photodamage. Main targetof photodamage is PSII, particularly its core protein D1 (Kyle et al., 1984; Mulo et al., 2008; Mellis, 1999). PSII repair machinery is situated in GM and SL (Suorsa et al., 2014). PSII repair cycle is described in chapter 2.2.7.

Under HL conditions, thylakoids undergo extensive architectural switches consisting of lateral shrinkage of grana diameter and increase of margins accompanied by lumen swelling (Herbstová et al., 2012; Kirchhoff, 2014; Puthiyaveetil et al., 2014), vertical unstacking of grana (Fristedt et al., 2015; Khatoon et al., 2009) and overall increased protein mobility in thylakoid membrane (Herbstová et al., 2012). All of these changes are believed to allow efficient PSII repair (Kirchhoff, 2013b).

2.1.4 Lumen

Thylakoid lumen is constricted and crowded continuous space enclosed by thylakoid membrane. Former assumptions that lumen is almost empty space containing PsbO, PsbP and PsbQ – PSII extrinsic proteins, electron carrier PC and violaxanthin de-epoxidase (VDE), protein involved in xanthophyll cycle turned to be wrong. According to proteomic and genomic data, up to 80 proteins are located in *Arabidopsis thaliana* lumen (Kieselbach et al., 1998; Peltier et al., 2002; Schubert et al., 2002). Hall et al. (2010) claim that more than 40 % of lumen proteome is redox regulated through modulation of disulfide bonds that control folding and/or enzyme activation.

Likewise thylakoid membrane subcompartments, also lumen undergo a light induced switch. In HL, an expansion of lumenal space occurs (reviewed in Mullineaux, 2005). It is linked to light-induced pH decrease from 7 in dark to 5–6 in light (Kramer et al., 1999; Cruz et al., 2001; Tikhonov, 2013) due to concomitant anion influx upon acidification (Kirchhoff et al., 2011). The luminal space increase probably allows better protein diffusion for PSII repair (Kirchhoff et al., 2011; and reviewed in Kirchhoff, 2013).

2.2 Photosystem II

Photosystem II is thylakoid membrane embedded, pigment–protein complex catalyzing water splitting and reduction of PQ (Vinyard et al., 2013).

2.2.1 Photosystem II function

Photosynthesis starts when photon is trapped by PSII, the first protein complex of electron transport chain. Light is absorbed by pigment molecules within antennae complexes and is transferred to reaction center (RC) consisting of D1, D2, CP43 and CP47 subunits. A special molecule of Chl *a* (P680) in RC is the place where charge separation occurs. Highly oxidative RC is used to drive water oxidation which take place in OEC. P680 which acts

as oxidation trap is converted to a reducing agent upon excitation (P*). P* reduces several molecules in stepwise manner, electron eventually reduce PQ to PQH_2 molecule (2 electrons are needed) which is the first mobile electron (and proton) transporter in photosynthetic machinery and migrates towards Cyt *b*6*f* (reviewed in Barber, 2012).

2.2.2 Photosystem II structure

An investigation of spinach revealed supramolecular structure of PSII-LHCII supercomplex in high resolution of 3.2 Å. This structural model consists of: 25 protein subunits, 105 Chl, 28 Car and other factors. Three extrinsic subunits form a triangular crown covering manganese cluster binding domains of CP43 and D1. The abovementioned structural characteristics were published by Wei et al. (2016) earlier this year.

PSII monomer/core complex (C) forms homodimer (C_2). Homodimer binds various number of LHCII, assembly is called supercomplex (SC). In thylakoids, several types of supercomplexes can be detected. Depending on the number of LHCII bound, C_2S_2, C_2S_2M or $C_2S_2M_2$ is formed, S – strongly, M – moderately bound. SC can further associate to each other and form so called megacomplexes – dimeric supercomplexes. Under specific condition (e.g. low light, response to cold stress), semi-crystalline macrodomains in the grana regions are formed (Boekema et al., 2000; Kouřil et al., 2011; Goral et al., 2012; reviewed in Dekker and Boekema, 2005 and Kouřil et al., 2012). Detailed PSII core structure regarding protein subunits is described in chapter 2.2.4.

2.2.3 Light harvesting complexes II

Light harvesting complexes II (LHCII) are pigment-protein complexes allowing (i) sunlight harvesting and energy transfer to reaction centers of PSII and (ii) photoprotection. During evolution, phycobilisomes found in cyanobacteria and some algae were substituted by LHC which is general term representing LHCI (PSI binding complexes) and LHCII (PSII

binding complexes). Unlike the evolutionary conserved core complex of PSII, LHCII are diversified group (Alboresi et al., 2008).

Antennae proteins, how LHCs are also called, are integral part of thylakoid membrane. They consist of three membrane spanning regions and carry Chl and Car molecules. The protein itself works as scaffold for pigments (Niyogi, 1999). Major (trimeric) LHCII consists of various combinations of three subunits: Lhcb1, Lhcb2, Lhcb3. Subunits Lhcb1and Lhcb2 combine to homotrimers or form Lhcb1, Lhcb2, Lhcb3 heterotrimers (Standfuss and Kühlbrandt, 2004). Subunits consist of three transmembrane regions A, B, C connected by both stroma and lumen exposed loops (Liu et al., 2004). Except subunits Lhcb1, Lhcb2 and Lhcb3, also monomeric antennae proteins Lhcb4 (CP29), Lhcb5 (CP26), Lhcb6 (CP24; Jansson, 1999), Lhcb7 (Klimmek et al., 2006) are to be found in higher plants.

Moreover, several proteins phylogenetically related to antennae are present. PsbS is not involved in light harvesting but is needed for non-photochemical quenching (NPQ), photoprotective mechanism which dissipate excess energy into heat (Li et al., 2000), early light-inducible proteins (ELIPs; Adamska et al., 1993), stress enhanced proteins (SEPs; Heddad and Adamska, 2000) and one helix proteins (OHPs; Jansson et al., 2000).

Among other pigments, one xanthophyll molecule which cycles through several forms is bound. Particular forms of this xanthophyll are able to dissipate excess of energy into heat (NPQ). This so called xanthophyll cycle is important in photoprotection (Liu et al., 2004).

LHCII are not irreversibly bound to PSII, on the contrary LHCII undergo redox-regulated phosphorylation, process on the basis of functional re-association between PSII and PSI upon light, so called “state transitions” (Allen et al., 1981; reviewed in Allen and Forsberg, 2001).

2.2.4 Intrinsic subunits

Monomer of higher plant PSII contains core complex consisting of four major subunits, namely D1 (PsbA), D2 (PsbD), CP47 (PsbB) and CP43 (PsbC) proteins, and twelve

low-molecular-mass membrane spanning protein subunits (PsbE, PsbF, PsbH, PsbI, PsbJ, PsbK, PsbL, PsbM, PsbTc, PsbW, PsbX and PsbZ; Wei et al., 2016).

Interestingly, all four major subunits show both high amino acid sequence conservation as compared to cyanobacteria *Thermosynechococcus vulcanus* and well conserved core complex cofactor binding sites. Low-molecular-mass subunits surround the major subunits by discontinuous belt-like structure. Eleven of them have homologous counterparts in cyanobacteria (Umena et al., 2011), whereas the remaining one, PsbW subunit, is unique for higher plants and algae (García-Cerdán et al., 2011). Another exception regarding small subunits is PsbZ, the only subunit with two transmembrane helices (Wei et al., 2016).

Small subunits PsbTc, PsbL and PsbM have important role in PSII core complex dimerization. PsbK, PsbJ, PsbE, PsbF, PsbX stabilize the core, PsbW, PsbZ and PsbH mediate association of peripheral antennae with the core (Wei et al., 2016) and PsbE, PsbF form cytochrome b_{559} which protects PSII from photodamage (Shi and Schröder, 2004).

Periphery of the core is surrounded by internal antennae, two monomeric antennae (CP26 and CP29) associate with PSII core subunits CP43 and CP47, respectively (Wei et al., 2016).

Each PSII monomer carry numerous cofactors, such as Chl *a*/*b*, Car, haem, PQ and lipids. Core subunits bind 35 Chl *a* (Chl *b* is not present), 2 pheophytin and 8 β-carotene molecules. Small subunits are poor regarding to pigments, bind only 2 Car and 1 haem molecule (Wei et al., 2016). Each mentioned group also binds numerous lipids which are not listed.

2.2.5 Oxygen evolving center

Light-induced water oxidation takes place in oxygen evolving center (OEC). OEC is located on the luminal side of PSII and consists of inorganic Mn_4CaO_5 cluster ligated by PSII core subunits D1 and CP43 (Ferreira et al., 2004). Extrinsic PSII subunits stabilize and protect cluster from exogenous environment and bind of Ca^{2+} and Cl^- needed for optimal water oxidation (reviewed in Aro, 2007; Roose et al., 2016).

Mn_4CaO_5 cycles through several redox states (S-states) on extraction of each electron by the RC of PSII. Two molecules of water are needed to produce four electrons and one molecule of oxygen (Kok et al., 1970; Joliot, 2003).

2.2.6 Extrinsic subunits

Optimal oxygen evolution requires several extrinsic proteins bound on the lumenally exposed surface of PSII. PsbO, PsbP, PsbQ and PsbR, the extrinsic proteins of PSII in higher plants, facilitate water oxidation along with extensive lumen protruding domains of intrinsic D1, D2, CP43 and CP47 subunits (Bricker et al., 2012). In contrast to chloroplast genome coded PSII core subunits (Shinozaki et al., 1986), in higher plants all four extrinsic proteins are coded in nuclear genome (Allahverdiyeva et al., 2013). Except for PsbR, extrinsic proteins are present in two isoforms in *Arabidopsis* genome (Allahverdiyeva et al., 2013). Chapters 2.3 and 2.4 are dedicated to PsbO, therefore it is not described here along with other extrinsic proteins.

PsbP subunit seems to be essential in binding of Ca^{2+} and Cl^- (Bricker and Frankel, 2011). There are also evidences that PsbP1 but not PsbP2 is essential for photoautotropic growth (Allahverdiyeva et al., 2013). In the same work was observed that PsbP levels in wt significantly decreased in older plants. Authors concluded that major role of PsbP is PSII and OEC assembly in early stages of plant development rather than its structural role in OEC stabilization. Yi et al. (2009) reported extensive architectural defects in RNAi suppressed expression (13 % and <1 % of wt protein levels) of PsbO genes. This observation highlights PsbP function in maintaining proper overall grana architecture.

Role of PsbQ is still quiet unclear, its absence has no effect on photoautotrophic growth under growth light (GL) conditions (Ifuku et al., 2005; Allahverdiyeva et al., 2013). Low light conditions caused strong phenotype of RNAi suppressed plants that eventually died (Yi et al., 2006). This observation may be explained by results of Allahverdiyeva et al. (2013) that in double mutant completely lacking PsbQ only about 50 % of the PSII–LHCII supercomplexes compared to wt was observed. PsbQ requirement for efficient supercomplex formation may be essential for plant growth under low light when the light is limited.

Only little is known about PsbR originally described as extrinsic subunit more than thirty years ago (Ljungberg et al., 1984). Model based on protein crosslinking and mass spectrometry was presented, where PsbR is located between PsbP and intrinsic PSII subunit PsbE (Ido et al., 2014). *A. thaliana* mutant *psbr* was used in order to investigate PsbR role in PSII. Mutant exhibited severe reductions of both PsbP and PsbQ level (3 % and 18 % of wt), but still was able to grow photoautotrophically (Allahverdiyeva et al., 2013). These findings imply that PsbP, PsbQ and PsbR work in concert.

Although new important findings in function and structure of PSII extrinsic subunits have been made in recent years, there are still many unknown facts regarding extrinsic subunits (Bricker et al., 2012).

2.2.7 Photosystem II repair cycle

Photosystem II repair cycle is considered to be one of the most efficient repair machineries in living organisms. PSII repair occurs with a half-time of about 1 hour (Neidhardt et al., 1998; Melis, 1999). Since PSII is photodamaged in all light intensities, considerable research focus is aimed to its repair and huge progress has been made recent years (reviewed in Järvi et al., 2015).

Repair cycle proceeds in stepwise manner consisting of disassembly of photodamaged complex, degradation, resynthesis and reassembly (Aro et al., 1993; Nixon et al., 2010; Nickelsen and Rengstl, 2013). Main target of photodamage is major subunit of core complex – D1 protein (Ohad et al., 1984). Active PSII is located mainly within stacked grana regions and *de novo* synthesis of D1 takes place in SL. Thus, damaged PSII have to migrate from crowded GC region through GM to SL (Kirchhoff et al., 2008).

To this day, generally accepted model (Fig. 4) of repair starts with PSII core protein phosphorylation catalyzed by kinase Stn8 (and possibly Stn7) which triggers disassembly of the supercomplex (Bonardi et al., 2005; Tikkanen et al., 2008). When PSII migrate to GM regions, complex is dephospohorylated by photosystem II core phosphatase (PBCP) and D1 is degraded by FtsH and DegP proteases (Samol et al., 2012; Puthiyaveetil et al., 2014).

De novo cotranslational synthesis of D1 most likely takes place in SL followed by reassembly in GM and/or SL (Puthiyaveetil et al., 2014).

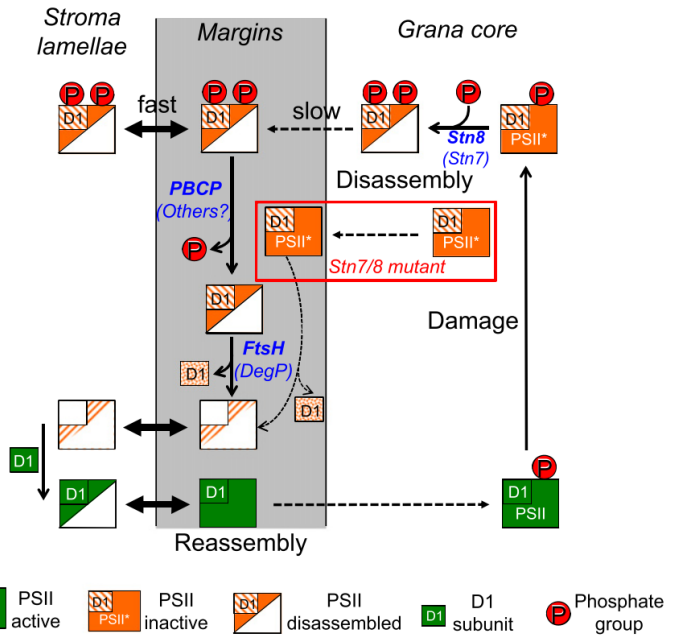

Figure 4. Photosystem II repair cycle scheme representing spatial segregation of particular enzymes and steps within thylakoid membrane subcompartments GC, GM and SL. (modified from Puthiyaveetil et al., 2014)

2.3 PsbO

PsbO, also called manganese–stabilizing protein or 33 kDa extrinsic protein, is fundamental for stabilization of Mn_4CaO_5 (OEC) cluster and oxygen evolution. Indispensable role of PsbO in oxygen evolution is supported by its presence among all oxygenic organism (De Las Rivas et al., 2004) and by cross-reconstitution experiments with PsbO isolated from cyanobacteria, red algae and higher plants (Enami et al., 2000).

2.3.1 Structure and interactions

PsbO is largest extrinsic subunit of PSII with molecular size of 26.5 kDa. Its size was formerly based on its SDS-PAGE mobility or on gel filtration, where it behaves as protein

of larger size of about 33 kDa (Abramowicz and Dismukes, 1984; Popelkova et al., 2002). It was reported, that unbound in solution it is natively unfolded or intrinsically disordered protein and exhibit extraordinary resistance to heat denaturation (Lydakis-Simantiris et al., 1999; Uversky et al., 2000). PsbO is also resistant to aggregation (as compared to bovine serum albumin or carbonic anhydrase), this feature seems to be highly important in crowded thylakoid lumen. Proper PSII-PsbO interaction is needed for efficient oxygen evolution (Wyman and Yocum, 2005). Moreover, it was shown that PsbO is able to undergo pH induced conformational changes (Shutova et al., 2005).

X-ray crystallography derived structure of cyanobacterial PsbO revealed that PsbO is elongated protein with two major domains (Fig. 5). Cylindrical domain I is formed by β-barrel protruding into lumen, domain II is extended head, in the vicinity of OEC, which forms a docking site to PSII (Ferreira, 2004; De Las Rivas and Barber, 2004).

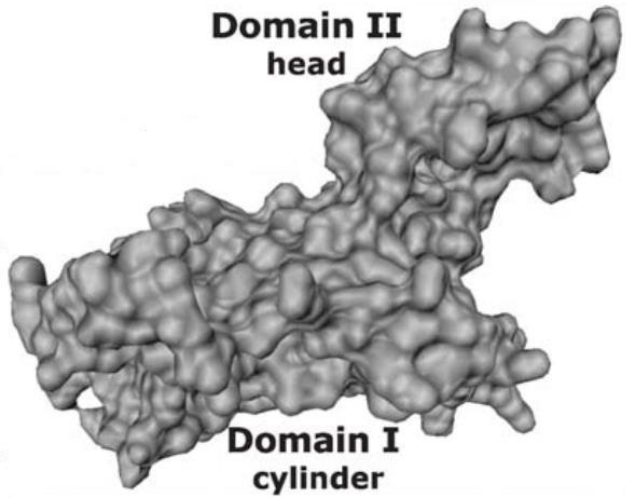

Figure 5. Structure of cyanobacterial PsbO derived from X-ray crystallography. PsbO is docked to PSII by its head domain II (modified from De Las Rivas and Barber, 2004)

Most extensive interactions between PsbO and PSII are formed with major core subunits D1 and CP43 however D2 and CP47 also participate. Therefore, all four major core subunits interact with PsbO. Interestingly, PsbO is also involved in interactions with CP47 subunit of other monomer of PSII dimer, this interaction probably helps to stabilize dimeric organization of PSII (De Las Rivas and Barber, 2004).

PsbO interactions with other extrinsic subunits were matter of debate for a long time (De Las Rivas et al., 2005; reviewed in Aro, 2007 and Roose et al., 2016). Structure of spinach PSII-LHCII supercomplex provided by Wei et al. (2016) revealed heterotrimeric triangular crown-like structure of PsbO, PsbP and PsbQ assembly (Fig. 6). PsbP binds near β-barel region of PsbO, particularly its β7- β8 loop, interaction is localized in canyon between luminal domains of CP43 and CP47. On the other side, PsbQ binds to N-terminal region of PsbO and simultaneously interacts with lumenal domain of CP43.

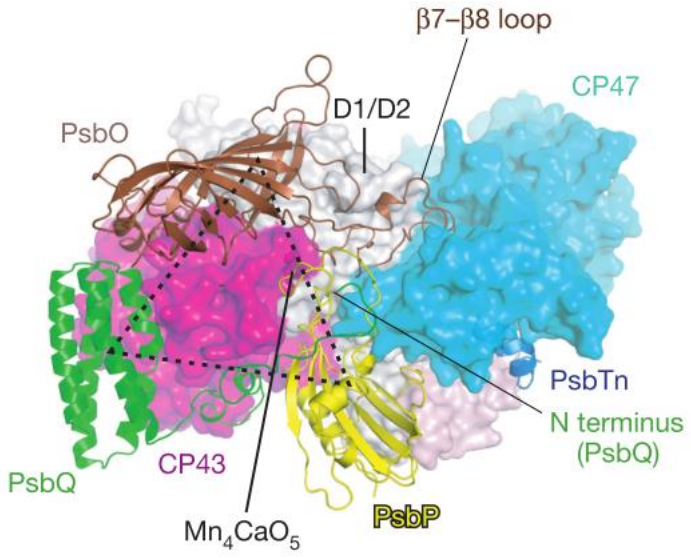

Figure 6. Triangular crow-like structure of photosystem II extrinsic subunits. Model is derived from crystallographic structure of PSII-LHCII supercomplex. Extrinsic subunit PsbR was not observed, on the other hand authors observed subunit PsbTn which has unknown function (modified from Wei et al., 2016)

2.3.2 Function

PsbO is fundamental for stabilization of Mn_4CaO_5 (OEC) cluster, although deletion of gene encoding PsbO protein in *Synechocystis* does not completely inactivate water oxidation (Mayes et al., 1991; Burnap and Sherman, 1991). Thus it is not absolutely essential for cyanobacterial photosynthesis. On the other hand, this *psbO*-less mutant was more sensitive to photodamage and could not grow in media containing low levels of Ca^{2+} and Cl^- (Philbrick et al., 1991; Komenda and Barber, 1995). Deletion of PsbO in eukaryotes leads to complete loss

of photosynthetic activity and ability to grow photoautotrophically as described for *Chlamydomonas reinhardtii* (Mayfield et al., 1987). No autotrophic mutant completely lacking PsbO has been obtained in higher plants (Murakami et al., 2005), which emphasize its indispensability in eukaryotes.

2.3.3 Stabilization of OEC

Variety of washing conditions of PSII preparations leads to selective removal of PSII extrinsic subunits. Removal of PsbO in most cases leads to destabilization of manganese cluster and release of Mn ions (Miyao and Murata, 1984; Bricker, 1992; Enami et al., 2000). This demonstrates its importance for water oxidation. Although PsbO stabilizes OEC cluster containing five metal ions, it is not directly involved in binding either of them and cannot be considered as metalloprotein (De Las Rivas and Barber, 2004).

Crystallographic studies revealed that N-terminus, C-terminus and β-barell are in quiet distance from the manganese cluster, while flexible loop of PsbO folds and assembles near to cluster (reviewed in Popelkova and Yocum, 2011). The sequence conservation of 37 members of PsbO family indicates that only 20 residues are fully conserved in all proteins. Detailed mapping showed that most of them are located in the backbone chain close to the regions of interaction with the OEC (De Las Rivas and Roman, 2005). Those observations indicate, that for stabilizing of OEC the flexible loop of PsbO is most important.

2.3.4 Other functions

Stabilizing of OEC and maintaining of oxygen evolution is the main and in evolutionary context the original function of PsbO. In recent years, several additional functions of PsbO were reported. Those functions might be specific for higher plants only (reviewed in Bricker and Frankel, 2011).

Spetea et al. (1999) reported that GTP bound to thylakoid membranes is needed for D1 degradation. More recently it was demonstrated, that PsbO is capable to bind GTP, therefore it was suggested, that PsbO-GTP binding is possibly related to D1 turnover (Spetea et al., 2004). The binding and hydrolysis of GTP might induce changes in conformation of PsbO and causes release from PSII (Lundin et al., 2007b).

Along with metal ions and Cl^-, also bicarbonate (HCO_3^-) is needed for optimal water oxidation. Investigation of pea PsbO brought interesting findings regarding to its carbonic anhydrase activity (Lu et al., 2005). The authors reported that PsbO but not PsbP and PsbQ are able to catalyze conversion of carbon dioxide into bicarbonate.

2.4 PsbO isoforms

Phylogenetic analysis provided by Duchoslav and Fischer (2015) revealed that many angiosperm families express two isoforms of PsbO.

2.4.1 Evolution

Phylogenetic analysis of 49 land plant species and 36 genera revealed that majority of analyzed angiosperms species express more than one isoform of *psbO* gene. Most of those species expresses two isoforms, species expressing more than two isoforms were assumed to be a result of recent genome duplications (Duchoslav and Fischer, 2015).

According to tree topology, Duchoslav and Fischer (2015) suggest that *psbO* duplication was facilitated by genome wide duplication (GWD) in ancestors of numerous families prior to species radiation. Therefore, two isoforms of *psbO* are not result of gene specific duplication but they were retained after GWD.

Mapping of the differences on the protein tertiary structure revealed that isoforms in individual species differ from each other on similar positions (Duchoslav and Fischer, 2015).

Mostly on the lumenally exposed end of β-barrel near the predicted GTP-binding site (Lundin et al., 2007b).

Duchoslav and Fischer (2015) hypothesize that isoforms evolution is based on "escape from adaptive conflict" scenario. Two isoform can specialize to specific functions which is obviously connected with losing in the other of the two functions.

2.4.2 Functions in *Arabidopsis thaliana*

Arabidopsis thaliana belongs to the group of angiosperms expressing two isoforms of *psbO* gene, namely PsbO1 and PsbO2. According to findings regarding *Arabidopsis* isoforms, it is obvious that they have different function. Mutants in either isoform are available, denoted as *psbo1* and *psbo2*, lacking PsbO1 and PsbO2 respectively. PsbO1 is the major isoform in wt plants (Murakami et al., 2005; Lundin et al., 2007a; Dwyer et al., 2012).

Plants *psbo1* show distinct phenotype with retarded growth and pale green leaves while *psbo2* seems not to be negatively affected under GL conditions (Murakami et al., 2002, 2005; Lundin et al., 2008; Allahverdiyeva et al., 2009). Exception is work of Lundin et al. (2007a) who observed phenotype also for *psbo2* in hydroponic cultivation. It seems that under GL, PsbO2 alone is not efficient in maintaining photosynthesis.

However, situation changed after exposure to long time (3 weeks) HL stress, all plants showed almost the same maximum quantum efficiency (F_v/F_m; Allahverdiyeva et al., 2009). Moreover, Lundin et al. (2007a) observed that *psbo2* has impaired D1 degradation, this highlights importance of PsbO2 under light stress. Lundin's et al. (2008) findings, that PsbO2 has higher GTPase activity than PsbO1 support the hypothesis that PsbO2 is involved in turnover of photodamaged D1 while PsbO1 facilitate efficient water oxidation (Lundin et al., 2008; Allahverdiyeva et al., 2009).

Therefore, presence of two PsbO isoforms most likely helps to adjust and optimize photosynthesis in response to light conditions (Duchoslav and Fischer, 2015).

3 Materials and Methods

3.1 Plant material

Arabidopsis thaliana wild type plants (Col 0) and T-DNA insertion mutants *psbo1* (SALK 093396) and *psbo2* (SALK 024720) obtained from The Nottingham Arabidopsis Stock Centre were used. At Charles University in Prague, Czech Republic, plants were grown in growth chambers in Jiffy-7 pellets (Jiffy, Kristiansand, Norway) with light/dark period 8/16 h, 100 μmol quanta·m^{-2}·s^{-1} at 23 °C. At Washington State University in Pullman, WA, USA, plants were grown in growth chambers in soil with light/dark period 9/15 h, 100 μmol quanta·m^{-2}·s^{-1} at 20 °C. Plants used for experiments were 7 weeks old.

3.2 Genotyping

Plants were screened for homozygosity by PCR using *psbO1* (forward: 5'–GGC CCA TTA GCT CAG TTG GT–3' and reverse: 5'–ACT CTG GAG GAG CGT TCT TG–3') and *psbO2* (forward: 5'–TCA CAC CCT ACT TGA ATT CAC CT–3' and reverse 5'–TTC GAG CCC ACT TCC TTC AC–3') gene specific sets of primers and universal primer for detecting T-DNA in Salk lines (5'–CTT GCT GCA ACT CTC TCA GG–3'). Primers were obtained from Generi Biotech (Hradec Králové, Czech Republic).

3.2.1 DNA isolation

Genomic DNA was isolated from freshly cut leaves. Immediately after cut, leaves were transferred to 2 ml Eppendorf tube, glass pellets were added and tube was frozen in liquid nitrogen. Leaves were homogenized in oscillating mill (MM 301, Retsch) for 5 min in frequency 25 Hz. Samples were shortly spun in centrifuge to remove material from the lid, 400 μl of extraction buffer (Tab. 1) was added and tube was thoroughly vortexed. 400 μl of chloroform was added and mixture was vortexed for 1 min. Tube was centrifuged at 13 800 × g for 3 min. 330 μl of the upper phase was transferred to new tube and 330 μl of isopropanol was

added, sample was well mixed and let stand on the bench for 2 min. Tube was then spun at 13 800 × g for 5 min, whole supernatant was carefully pipetted out and the pellet was dried at room temperature for 10 min. Pellet was dissolved in 100 µl of 2 mM Tris pH 8.5 buffer (Tab. 1).

Table 1 Buffers for DNA isolation

Buffer	**Composition**
Extraction buffer	200 mM Tris, 250 mM NaCl, 25 mM EDTA, 0.5 % SDS, pH 7.5 with HCl
Tris pH 8.5	2 mM Tris, pH 8.5 adjusted with HCl

3.2.2 PCR and agarose electrophoresis

Volume of samples for polymerase chain reaction (PCR) was 20 µl. Composition of mixture was following:

DNA	1 µl
10x buffer with $(NH_4)_2SO_4$	2 µl
25 mM $MgCl_2$	1.2 µl
10 mM dNTP	0.4 µl
10 µM primer 2x	0.4 µl
Taq polymerase	0.4 µl
Deionized water	14.6 µl

The PCR conditions: initial denaturation at 94 ºC for 5 min, denaturation at 94 ºC for 30 s, annealing at 57 or 59 ºC (depending on sets of primers) for 30 s, extension at 72 ºC for 1 min. Denaturation, annealing and extension step was repeated for 35 cycles.

Separation of PCR products was carried out by electrophoresis in 1.2 % agarose gel in TAE buffer (Tab. 2) with added GelRed™ (Biotium) for DNA visualization. Prior to loading, samples were mixed with BPB (Tab. 2) in ratio 5:1. As DNA ladder GeneRuler 100 bp

Plus DNA Ladder (Fermentas) was used. Samples were run in direct current (5 V/cm). Gels were visualized by G:BOX with UV light transiluminator from SynGene.

Table 2. Buffers for agarose electrophoresis

Buffer	**Composition**
50x TAE buffer	242 g Tris, 57.1 ml acetic acid, 100 ml 0.5 M EDTA (pH 8.0)
BPB buffer	0.025 % bromphenol blue (BPB), 30 % glycerol in 10 mM Tris, pH 7.8 adjusted with HCl

3.3 High light treatment

Dark adapted wt plants (after the 16 hours of dark period) were used for experiments with HL. Prior to exposure to excess of light, maximal photochemical efficiency of PS II (ratio of variable to maximum fluorescence, F_v/F_m) was measured with a pulse-modulated fluorimeter (Hansatech OxyLab).

Plants were transferred to FytoScope Chamber FS 130 (Photon Systems Instruments) with light intensity 1200 μmol quanta$\cdot m^{-2}\cdot s^{-1}$ and temperature 21 ºC. After treatment, plants were kept in dark for 3 – 5 min and F_v/F_m spectra was measured again. Plants were immediately used for further experiments as thylakoid or lumen isolation.

3.4 Thylakoid membranes isolation

Dark adapted plants (after 16 hours of dark period) were used for thylakoid isolation unless otherwise specified. All steps in process were carried out in dark on ice. Arabidopsis leaves from 2–3 plants were harvested by scissors, transferred to beaker, washed three times in distilled water and dried in paper towels. In cold room, leaves were transferred to blender and 50 ml of grinding buffer (Tab. 3) was added. Blender (Commercial blender 7011, Warning) was run three times for 3–5 s at low speed. Homogenate was filtered through 1 layer of miracloth, 8 layers of cheesecloth and paper towel. Filtered homogenate was spun at 2000 × g, 4 ºC for 2 minutes in glass tubes and supernatant was removed. Pellet was resuspended in 9 ml of shock buffer (Tab. 3) using fine brush, collected to plastic tube and incubated on ice for at least 10 minutes and from cold room transferred back to room temperature (RT).

After incubation, tube was spun at 23 500 × g 4 ºC for 10 minutes and supernatant was removed. Pellet was resuspended in small volume (1 ml) of storage buffer C (Tab. 3) with added protease and phosphatase inhibitors using fine brush and transferred to 2 ml microcentrifuge tube. Tube was spun at 1 500 × g, 4 ºC for 10 minutes. Supernatant was removed and pellet again resuspended in storage buffer C using fine brush, this washing step is to remove any residual shock buffer. Chlorophyll determination was carried out according to Porra et al. (1989).

Table 3. Buffers for thylakoid membranes isolation

Buffer	**Composition**
Grinding buffer	0.4 M Sorbitol, 20 mM Tricine, 10 mM EDTA, 10 mM $NaHCO_3$, 0.15 % BSA (w/v), pH 8.4 adjusted with KOH
Shock buffer	25 mM Hepes, 40 mM KCl, 7 mM $MgCl_2$, pH 7.5 adjusted with KOH
Storage C buffer	0.1 M Sorbitol, 50 mM Hepes, 2 mM $MgCl_2$, pH 7.5 adjusted with NaOH Proteases: 40 µM Leupeptin, 40 µM Antipatin, 0.4 mM Pefabloc Phosphatases: 10 mM NaF, PhosSTOP – 1 tablet (Roche)

3.5 Fractionation using digitonin

Fresh TH isolated as described above were used for digitonin fractionation. As for TH isolation, fractionation was done in dark. After chlorophyll determination, TH were transferred from ice to (RT) for 40–60 min. Digitonin works best at RT. TH were diluted to concentration of 0.6 mg Chl/ml and mixed with equal volume (usually 0.75 ml + 0.75 ml) of 2 % (m/m) digitonin solution dissolved in storage buffer C. Mixing was done in small flat bottomed tube using microstirrer bar spinning at moderate speed. Digitonin solution was added drop by drop by pipette. Mixture was incubated at RT for 10 minutes. After that content was transferred to microcentrifuge tube and immediately spun at 1000 × g, 4 ºC for 1 minute and since this moment kept on ice again. This spinning step was done to remove unsolubilized material (seen as small pellet at the bottom of the tube). Supernatant was transferred to a new tube and spun at 40 000 × g, 4 ºC for 30 minutes. Supernatant was carefully transferred to a new tube, pellet at the bottom was the grana core fraction. Pellet was resuspended in small volume (150 µl) of storage buffer C using fine brush. Supernatant was spun in ultracentrifuge at 140 000 × g, 4 ºC for 90 minutes. The clear supernatant was pipetted out and two pellets were visible in the tube. Solid round pellet collected

as stroma lamellae and loose pellet collected as grana margins. Loose pellet was transferred to a new tube and solid pellet was resuspended in small volume (120 µl) of storage buffer C. Chlorophyll concentration of individual fractions was determined and yield of fractions was calculated as Chl concentration multiplied by volume of sample. According to Puthiyaveetil et al. (2014), percentage of chlorophyll corresponds directly to the percentage of membrane for each thylakoid subcompartment. The Chl a/b ratio can be used as diagnostic of proper isolation of individual fractions. Ratios for particular fractions should be in range or close to following numbers: grana core 2.0 – 2.4, grana margins ~ 3.5 and stroma lamellae > 4.0 (Puthiyaveetil et al., 2014).

3.6 Lumen isolation

Leaves harvesting through homogenate filtration and first spinning were identical to TH isolation. Pellet was resuspended in 20 ml of grinding buffer (Tab. 3) using fine brush and spun again at 2 000 × g, 4 ºC for 2 minutes and supernatant was removed. Shock lumen buffer (Tab. 4) was added and pellet was resuspended using fine brush, chloroplasts were osmotically shocked

for 2 minutes, spun at 2 500 × g for 3 min and supernatant was removed. Pellet was resuspended in 1 ml of VDE buffer (Tab. 4), transferred to 2 ml microcentrifuge tube, spun at 1 500 × g, 4 ºC for 10 minutes and supernatant was removed. Pellet was again resuspended in VDE buffer (0.5 ml). Chlorophyll concentration was determined and adjusted to 2 mg Chl/ml. Thylakoids were frozen in liquid nitrogen and immediately thawed in water (29 ºC). Freeze – thaw step was made 7 times. Samples were spun at 38 000 × g, 2 ˚C for 20 minutes. Colourless supernatant containing luminal proteins was transferred to new tube.

Table 4. Buffers for lumen isolation

Buffer	**Composition**
Shock lumen buffer	10 mM MES, 5 mM $MgCl_2$, 10 mM NaCl, pH 6.5 adjusted with NaOH
VDE buffer	20 mM Tris, 5 mM $MgCl_2$, pH 7.5 adjusted with HCl

3.7 Luminal protein determination

Luminal protein determination was made with Pierce BCA Protein Assay Kit (Thermo Scientific). Dilution series of bovine serum albumin (BSA) standards was prepared according to protocol. Working reagent (WR) was prepared by mixing 50 parts of BCA Reagent A with 1 part of BCA Reagent B (50:1, Reagent A:B).

Procedure was made in 96 well microplate, to each well was added 200 µl of WR and 25 µl of standards or sample. Plate was then mixed on vortex for 30 s and incubated at 37 ºC for 30 min. After cool down to RT absorbance was determined spectrophotometrically at 562 nm wavelength on plate reader.

3.8 Blue-Native electrophoresis

3.8.1 Gel preparation

Blue-Native PAGE is a method which uses gradient gels for separation of natively folded protein complexes. Ethanol washed glass plates with no wedges and 1 mm thick spacers were used. Glass plates were mounted to the holder and sealed with a mixture of 40 µl 10 % APS and 2 ml "Plug" solution (Tab. 7) and immediately poured between the glass plates. Acrylamide (AA) solutions were prepared without TEMED and APS (Tab 5).

Table 5. Composition of acrylamide gels for gradient gel preparation.

	12 % AA	**6 % AA**
Acrylamide (30/0.8)	5.6 ml	2.8 ml
6x Gel buffer	2.33 ml	2.33 ml
Glycerol (p.a.)	2.8 g	-
H_2O dist.	4 ml	8.87 ml
TEMED	6.67 µl	6.67 µl
APS (10 % w/v)	26.7 µl	26.7 µl
Total volume	**14 ml**	**14 ml**

Before filling the gradient maker, the stirrer in the right hand side chamber (12 % AA) was adjusted to high speed and turned off. APS and TEMED were added to the 6 % AA solution, vortexed thoroughly, filled into the left chamber and the tunnel between chambers was filled to avoid bubbles in gel. 12 % AA solution was thoroughly vortexed in order to completely dissolve glycerol, filled into the right chamber, and APS and TEMED were added. Stirring was immediately turned on. First the outlet valve was opened and immediately the chamber connecting valve was opened too. This avoided premixture of the two solutions before casting the gel. After the casting was finished, the gel was overlaid with 3–4 ml of isopropanol. Polymerization took 1–2 hours. When the gel was polymerized, the isopropanol was removed and the gel was rinsed with distilled water several times until all the isopropanol smell was completely removed. Any residual water was removed with 1 mm thick Whatman paper. Stacking gel solution was prepared according to Tab. 6. The stacking gel was poured onto gradient gel and comb was added. Polymerization of stacking gel took around 1 hour.

Table 6. Composition of 4 % stacking gel for BN-PAGE

	4 % AA
Acrylamid (30/0.80 6 Gel buffer H_2O dist.	1.6 ml 2 ml 8.27 ml
TEMED APS (10 % w/v)	12 µl 120 µl
Total volume	**12 ml**

Table 7. Buffers and solutions for Blue-Native PAGE casting

Buffers and solution	**Composition**
6x Gel buffer*	750 mM ε-ACA**, 1 M Bis-Tris, pH 7.0 adjusted with HCl
"Plug" solution	5 ml H_2O, 4 ml Acrylamide (30/0.8), 45 µl TEMED
10 % APS	1 g Ammonium persulfate in 10 ml water, stored at -20 ºC

* store at 4 ºC, ** ε-ACA = ε-Aminocapronic acid

3.8.2 Solubilization of membrane membranes for blue-native PAGE

Thylakoid membranes isolated as described above were solubilized with detergent prior to loading on the gel. All steps were made in dark and on ice. Two aliquots of each sample with amount of chlorophyll 50 µg each were taken. 300 µl of TMK buffer (Tab. 8) was added to each sample. Samples were spun at 2 320 × g, 4 ºC for 2 minutes. Supernatant was removed by pipette and pellet was resuspened in 300 µl of TMK buffer. Washing step was repeated. Supernatant was removed and pellet was resuspended in 60 µl of ε-ACA buffer (Tab. 8). 6 µl of 10 % dodecyl α-D-maltoside were added, sample was vortexed for 1 s to homogenize the mixture and incubated on ice for 10 minutes. Sample was then spun at 15 700 × g, 4 ºC for 10 minutes, nonsolubilized material was visible in the pellet. Supernatant was carefully transferred to a new tube. 6 µl of Coomassie loading buffer (Tab. 8) was added, vortexed for 1 s and incubated on ice for 10 minutes.

Table 8. Buffers and solutions for thylakoid membranes solubilization

Buffers and solutions	**Composition**
TMK buffer	10 mM Tris, 2 mM $MgCl_2$, 20 mM KCl, pH 6.8 adjusted with HCl
ε-ACA buffer	750 mM ε-ACA, 50 mM Bis-Tris, 5 mM EDTA, 50 mM NaCl, pH 7.0 adjusted with HCL
Coomassie loading buffer	750 mM ε-ACA, 5 % Coomassie-G
10 % Dodecyl α-D-maltoside	10 % solution of Dodecyl α-D-maltoside in water, stored at -20 ºC, thawed only once

3.8.3 Running Blue-Native PAGE

Blue native electrophoresis was carried out in a cold room (4 ºC). 2 liters of 1x anode buffer (Tab. 9) were added to the main (big) chamber of the apparatus. Gel was fixed to appropriate chamber, apparatus was completed and the whole assembly was transferred to the cold room. Blue cathode buffer (Coomassie added, Tab. 9) was added to the upper chamber and gel pockets were washed with a syringe. Samples were loaded, two technical replicates each. Gel was run overnight (50 V). Next day in the morning when the blue cathode buffer reached

1/2 – 2/3 of the overall size of the gel was changed for colorless cathode buffer. The upper part of the 4 % stacking gel was removed. Gel was run at 250 V for 4 more hours, until the dye reached the bottom of the gel.

Glass was disassembled, rest of the stacking gel and the bottom part of the gel were cut out. Gel was transferred to bowl with distilled water and was scanned.

Table 9. Buffers for Blue-Native PAGE run

Buffers	**Composition**
Anode buffer	50 mM Bis-Tris, pH 7.0 adjusted with HCl
Cathode buffer	50 mM Tricine, 15 mM Bis-Tris, 0.02 % Coomassie-G*, pH 7.0 adjusted with HCl

*pH was adjusted before adding Coomassie-G, 1x buffer with Coomassie and 1x without Coomassie-G were prepared

3.9 Nonstructural saccharides (NSS) content determination

NSS content determination was done by Dr. Lipavska's team in Laboratory of Plant Morphogenesis Regulating Factors, Department of Experimental Plant Biology, Faculty of Science, Charles University in Prague, Czech Republic.

3.9.1 Soluble saccharide content determination

Leaf samples from 7 weeks old, 16 hours DA plants were cut, immediately weighed (50-60 mg each replicate), freeze-dried and dry weights were determined. The dried material was homogenized by shaking with glass beads (3 mm diameter) and boiled with 80 % methanol (0.5 ml) at 75 ºC for 10 min. The solvent was evaporated and the residue was dissolved in double-distilled water in an ultrasonic bath for 10 min. The samples prepared for sugar determination were stored after filtration using 0.45 µm membrane filters (Whatman) at -18ºC (Lipavska and Vreugdenhil, 1996). The content of extracted soluble NSS was detected using high-performance liquid chromatography (HPLC) with refractometric detection (Spectra Physics;

refractometer Shodex RI-71; integrator ChromJet; pre- column Hema-Bio 1000 Q + SB, Watrex, Czech Republic; column Hi Plex Ca^{2+}, Polymer Laboratories, U.K.; eluent ultrapure water MilliQ, Millipore; isocratic pump, Spectra Physics; flow rate: 0.5 ml min^{-1}, temperature 80 ºC; volume of injected sample 10 µl).

3.9.2 Starch content determination

For starch content determination, the same types of samples as for soluble NSS content determination were taken. Samples frozen in liquid nitrogen were freeze-dried and dry weight was determined. The material was homogenized by shaking with glass beads (3 mm diameter) and boiled with 80 % methanol (0.5 ml) at 75 ºC for 10 min. The methanol was evaporated and the residue was washed in double-distilled water in an ultrasonic bath for 10 min. Samples were centrifuged, the pellet was washed once more in the same way, then the water was evaporated. After addition of 0.5 ml of 0.1 M acetate buffer, pH 4.5, pellets were boiled for 10 min. Samples were incubated at 55 ºC for 4 h with 60 IU of amyloglucosidase (Rhizopus, Sigma), vacuum-dried, and solids resuspended in 0.5 ml double-distilled water in an ultrasonic bath for 10 min. The samples prepared for glucose content determination were stored after filtration using 0.45 pVm membrane filters (Whatman) at -18 ºC. The extracted glucose content was detected using HPLC as above.

Procedures described in chapters 3.9.1. and 3.9.2. were taken from Lipavska et al. (2000).

3.10 Difference absorption spectroscopic cytochrome b_{559} determination

Spectroscopic determination of integral PSII protein subunit cyt b_{559} was made with Hitachi U3900 spectrometer using software UV solutions. Baseline was established with DA buffer (Tab. 10) containing 0.18 % *n*-Dodecyl β-D-maltoside (β-DM) and buffer was thoroughly removed from cuvette with syringe. Reaction mixture was composed of DA buffer containing a sample in concentration of 40–50 µM Chl with overall volume of 500 µl. 1 µl of 1 M FeCN

(Tab. 10) was added to microcentrifuge tube with reaction mixture, thoroughly mixed by pipette, transferred to cuvette, put to instrument and incubated for 1 min and then measured (9 times and averaged). FeCN has positive redox potential to oxidize everything, oxidized state is then measured. 5 µl of 1 M Sodium Ascrobate (Tab. 10) was added and mixed with glass Pasteur pipette, put to instrument, incubated for 2 min and measured same as described above. With ascorbate high potential of cyt b_{559} is measured. Several grains of dithionite were added and carefully mixed with Pasteur pipette. A layer of paraffin (50 µl) oil was put on the surface of the mixture, cuvette was put to instrument and incubated for 5 min and measured. Dithionite reacts with oxygen to acid, due to this, it is necessary layer surfaced with paraffin oil. With dithionite, low potential of cyt b_{559} is measured. Raw data were processed with Sigmaplot 11 (Systat Software Inc.) software.

Table 10. Buffers and solutions for cytochrome b_{559} determination

Buffers and solutions	**Composition**
DA (diff. absorption) buffer*	20 mM HEPES, 330 mM sorbitol, 10 mM KCl, 50 µM EDTA, pH 7.6 adjusted with NaOH
Sodium ferrocyanide	1 M (65.824 mg/0.2 ml)
Sodium ascorbate	1 M (39.64 mg/0.2 ml) prepared fresh and kept on ice

* β-DM was added before use

3.11 SDS-Urea-PAGE

Denaturating polyacrylamide gel electrophoresis was made with SE 260 mini-vertical gel electrophoresis unit (GE Healthcare Life Sciences) in 0.75 mm thick, 7 cm long, 11% AA, 6 M urea gels.

3.11.1 Gel preparation

Gel for SDS-Urea-PAGE was prepared according to Tab. 11 and 12. Both mixtures were prepared simultaneously except addition of APS and TEMED. Mixtures were thoroughly vortexed and APS and TEMED were added to resolving gel, mixture was poured between glass plates. Immediately

after that, APS and TEMED was added to resolving gel and poured between glass plates, comb was added. Polymerization took 40 – 60 min.

Table 11. Composition of SDS-Urea polyacrylamide gel

	Resolving gel 1x	**Stacking gel 1x**
AA/Bis 40 %	1306 µl	263 µl
dd H2O	567 µl	1450 µl
Separating buff.	1300 µl	-
Stacking buff.	-	250 µl
Urea	1.62 g	-
10 % SDS	45 µl	20 µl
10 % APS	30 µl	15 µl
TEMED	4 µl	3 µl
Total:	**4.5 ml**	**2 ml**

Table 12. Buffers for SDS-PAGE

Buffers	**Composition**
Separating buffer	1.5 M Tris, pH 8.8 adjusted with HCl
Stacking buffer	1.0 M Tris, pH 6.8 adjusted with HCl

3.11.2 Sample preparation

Volume containing 1 µg of chlorophyll (approximately corresponds to 5 µg of protein) for TH, GC, GM and SL or 3 µg of proteins for lumen was taken. The sample was mixed with equal volume of 2x sample buffer (S.B., Tab 10) and with 1x S.B. to reach total volume of 10 µl for TH, GC, GM and SL or 38 µl for lumen. The sample was boiled for 5 minutes and spun at 16 000 × g for 1 min.

Amersham ECL High-Range Rainbow Molecular Weight Marker (GE Healthcare Life Sciences) was mixed with 1x S.B. in ratio 1:1 (5 µl + 5 µl). As blank 10 µl of 1x S.B. was used.

Table 13. Buffers for SDS-PAGE sample preparation

Buffers	Composition
5x Sample buffer*	220 mM Tris-HCl pH 7.5, 10 % β-mercaptoethanol, 12.5 % SDS, 0.05 % bromphenol blue (BPB), 45 % glycerol,

*Diluted to 2x before use

3.11.3 Running denaturating gel

Gel was fixed to apparatus, upper and bottom chambers were filled with 1x running buffer (SDS added, Tab. 14). Pockets were washed using 1 ml pipette and samples were loaded with gel loading tip. Electrophoresis usually ran for 2.5 – 3 hours at 12 – 14 mA.

Table 14. Buffers for SDS-PAGE run

Buffers	Composition
Running buffer	25 mM Tris, 250 mM glycine*, 0.1 % SDS

* ELFO grade pH 8.3

3.12 Western Blot

Arabidopsis thaliana isoform specific antibodies were obtained from Agrisera, Sweden (anti-PsbO1 AS14 2824 and anti-PsbO2 AS14 2825). Antibodies are derived from location after amino acid 180 of PsbO isoforms (personal communication with Joanna Porankiewicz-Asplund, Agrisera), therefore closer to the C-terminus, region differing only in 3 amino acids between isoforms. Anti-D1 protein antibody raised against C-terminus used in experiments was also obtained from Agrisera.

3.12.1 Blotting

Directly after electrophoresis, gel was rinsed with water and glass plates were disassembled, stacking gel and bottom part of resolving gel was cut out. Gel was carefully transferred to bowl and washed in distilled water 3 times, then blotting buffer (Tab. 15) was added for 5 – 10 minutes. PVDF membrane was activated for 1 min in methanol and washed in distilled water 3 times,

blotting buffer was added for at least 10 minutes. Two pieces of filter paper and two fiber pads were soaked in blotting buffer in a glass bowl. In another bowl, gel holder cassette was laid and gel sandwich was prepared in following order: cassette (black side down), fiber pad, filter paper, gel, PVDF membrane, filter paper, fiber pad. Cassette was carefully closed and placed into a cassette holder in apparatus. Blotting buffer (1 liter) and ice cooling unit was added to apparatus and closed. Blotting was made at 350 mA for 1 hour. Mini Trans-Blot® Cell (Bio-Rad) apparatus was used.

3.12.2 Blocking

After 1 hour of blotting the cassette was moved out, opened and membrane transferred to bowl with 5 % milk in TBS-T buffer (blocking solution. Tab. 15). Membrane was blocked overnight in a cold room on a shaker adjusted to gentle speed.

3.12.3 Antibodies incubation

Next day in the morning, membrane was washed in TBS-T buffer (Tab. 15) 3 times for 5 min in RT on orbital shaker. After last washing step, membrane was gently dried on paper towel to remove any residual buffer to avoid diluting of antibodies. Membrane was cut to two pieces when both isoforms were detected on one membrane and each piece was incubated separately. Antibodies were used in dilution of 1:1000. Incubating time was 1.5 hour for PsbO antibodies and 1 hour for D1 antibody in bowls covered with aluminum foil on orbital shaker. Primary antibodies were used repeatedly and stored in -20 ºC. Membrane was gently rinsed in TBS-T buffer, washed 3 x 5 min and 1 x 15 min in the same buffer. Secondary antibody (anti-rabbit) was used in dilution of 1:50 000 for 2 hours. Secondary antibody was used only once. Membrane was washed in the same wash steps as described above, after last step buffer was removed.

3.12.4 Detection

Detection of proteins was carried out with ImmunoCruz™ Western Blotting Luminol Reagent: sc-2048 (Santa Cruz Biotechnology). Mixture was prepared by mixing 0.75 ml of reagent A + 0.75 ml of reagent B in dark. Mixture was kept in a falcone tube covered in aluminum foil. Following procedure was all done in a dark room. Three bowls were prepared (developer, fixer, water). Reagent mixture (A+B) was added to bowl containing membrane and incubated for 1 min. Then the mixture was removed and membrane gently dried on a paper towel. Membrane was placed between two layers of plastic foils and to a cassette for membrane incubation. A sheet of film was placed onto membrane and the cassette was closed. Incubating times were usually around 10 s. Film was immediately transferred to developer – washed in water – fixer – washed in water and dried on air in RT. Membrane was stained in Amido black solution (Tab. 15) for 1 min, washed in water several times and dried on air in RT as well. Dry blots were scanned and densitometrically quantified with ImagePro (Media Cybernetics Inc.) software.

Table 15. Buffers and solution for western blot

Buffers	**Composition**
10x TBS buffer*	100 mM Tris, 1.5 M NaCl, pH 7.6 adjusted with HCl
TBS-T buffer	100 ml 10x TBS, 0.5 ml Tween 20, filled to 1 liter with distilled water
Blotting buffer	25 mM Tris, 192 mM Glycin
Blocking solution	TBS-T with 5 % w/v nonfat dry milk (Bio-Rad), 20 ml for one membrane
Amido black	MeOH 20 ml, acetic acid 5 ml, amido black 50 mg, adjusted with water to 50 ml

*Diluted to 1x TBS before to use

3.12.5 Western blot data normalization

Samples obtained by fractionation were loaded on gel in two different orders. Fractions from given fractionation were loaded and detected by WB for each fractionation. In the second order of loading, only one particular fraction was loaded in all treatments (DA, 1h HL, 2h HL)

and all biological replicates with the aim of seeing changes on timescale. Thus, two densitometric quantifications were done for each sample. This allowed to normalize all WBs to each other. For normalization, MS Office Excel with Solver extension was used.

4 Results

4.1 Characterization of *psob1* and *psbo2* mutants

4.1.1 Selection of *psbo1* and *psbo2* homozygous plants

In this study, two *Arabidopis thaliana* T-DNA insertion mutant lines in each of the two *psbO* genes and wildtype (wt, ecotype Columbia-0) were used. Mutants are denoted as *psbo1* and *psbo2*, with T-DNA insertions in genes *psbO1* and *psbO2*, respectively. Mutants were obtained from The Nottingham Arabidopsis Stock Centre as heterozygous seeds. In order to select homozygous plants only, presence of T-DNA insertions in plants grown from obtained seeds was confirmed by PCR. Two combinations of primers were used for each mutant line: (1) gene specific primer with T-DNA specific primer and (2) two gene specific primers. To confirm T-DNA insertions in mutants, PCR with T-DNA specific primer in combination with *psbO1* or *psbO2* gene specific primer was carried out for *psbo1* and *psbo2* mutant respectively. Second PCR was carried out to confirm that respective gene is not present. Mutants were screened with a pair of *psbO1* and a pair of *psbO2* gene specific primers for *psbo1* and *psbo2* mutant respectively (Fig. 7).

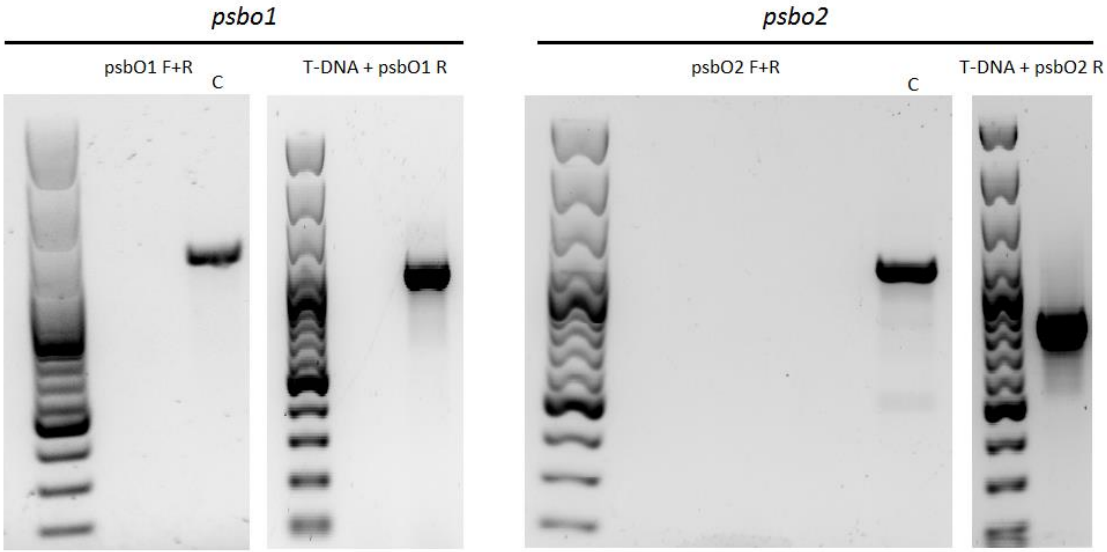

Figure 7. Selection of homozygous *psbo1* and *psbo2* mutants. Positive controls are denoted as C.

4.1.2 Phenotype of *psbo1* and *psbo2* mutant plants

The *psbo1* mutant showed pronounced phenotype with retarded growth rate, significantly reduced rosette size and pale green leaves in comparison with wt. The *psbo2* mutant was not different from wt plants in any of these characteristics (Fig. 8 and 9).

Figure 8. *A. thaliana psbo1*, *psbo2* and wt plants grown at Washington State University. Plants were 7 weeks old.

Figure 9. *A. thaliana psbo1*, *psbo2* and wt plants grown at Charles University. Plants were 7 weeks old.

Experiments for this study were carried out in two places. At Charles University in Prague, Czech Republic, plants were grown in growing chambers in jiffy pellets with light/dark period 8/16 h, 100 μmol quanta·m^{-2}·s^{-1} at 23 °C. At Washington State University in Pullman, WA, USA, plants were grown in growing chambers in soil with light/dark period 9/15 h, 100 μmol quanta·m^{-2}·s^{-1} at 20 °C. Phenotype of *psbo1* mutant was even more pronounced (smaller plants) in plants grown in USA.

In addition, plants grown at Washington State University, Pullman, USA looked different as compared to plants grown at Charles University, Prague, Czech Republic. In Pullman, plants exhibited compact rosette with short petioles while in Prague exhibited leaves with long petioles and loose rosette.

Mutant plants *psbo1* and *psbo2* showed significant decrease (Fig. 10) in ratio of dry weight (DW)/fresh weight (FW) compared to wt. Dry weight is expressed in percent of fresh weight: 13.7 ± 0.36 %, 6.27 ± 0.16 %, 12.04 ± 0.39 % for wt, *psbo1* and *psbo2* respectively. Mutant *psbo2* is just a bit lower than wt, while *psbo1* exhibited less than half of wt ratio.

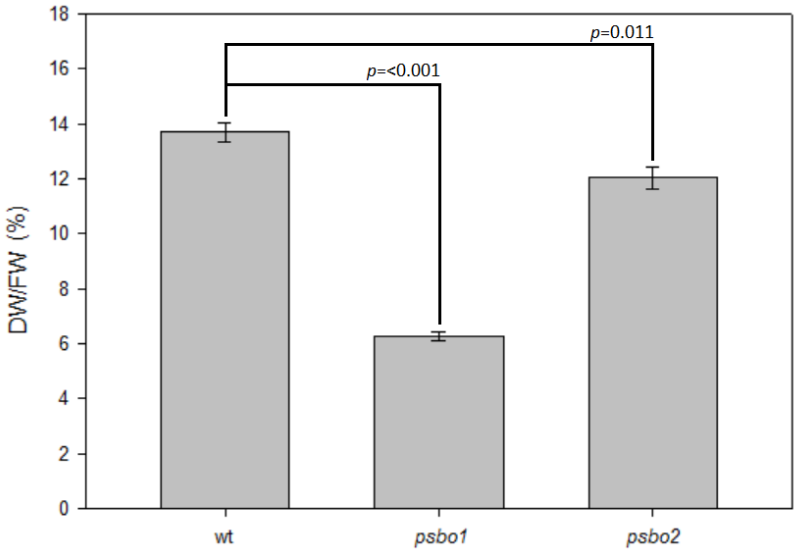

Figure 10. Ratio of dry weight/fresh weigh (DW/FW) expressed in percent. Both mutants showed significant decrease. Means and SE are calculated from six biological replicates.

4.1.3 Immunology assays

4.1.3.1 Antibody specificity control

As the initial step, specificity of antibodies was confirmed by western blot (WB). TH from both mutants and wt plants, protein amount corresponding to 1µg of Chl, were separated by SDS-PAGE, proteins were blotted on PVDF membrane and PsbO proteins were detected. Antibodies showed specificity without cross-reactions in mutants. Treatment with antibody against PsbO1 detected band in sample from *psbo2* and wt but no signal in *psbo1*. Analogously antibody against PsbO2 detected band in sample from *psbo1* and wt and no signal in size corresponding to PsbO in sample from *psbo2* (Fig. 11). Besides the specific interaction of antibody against PsbO2, on some blots a nonspecific band with size about 50 kDa was also visible.

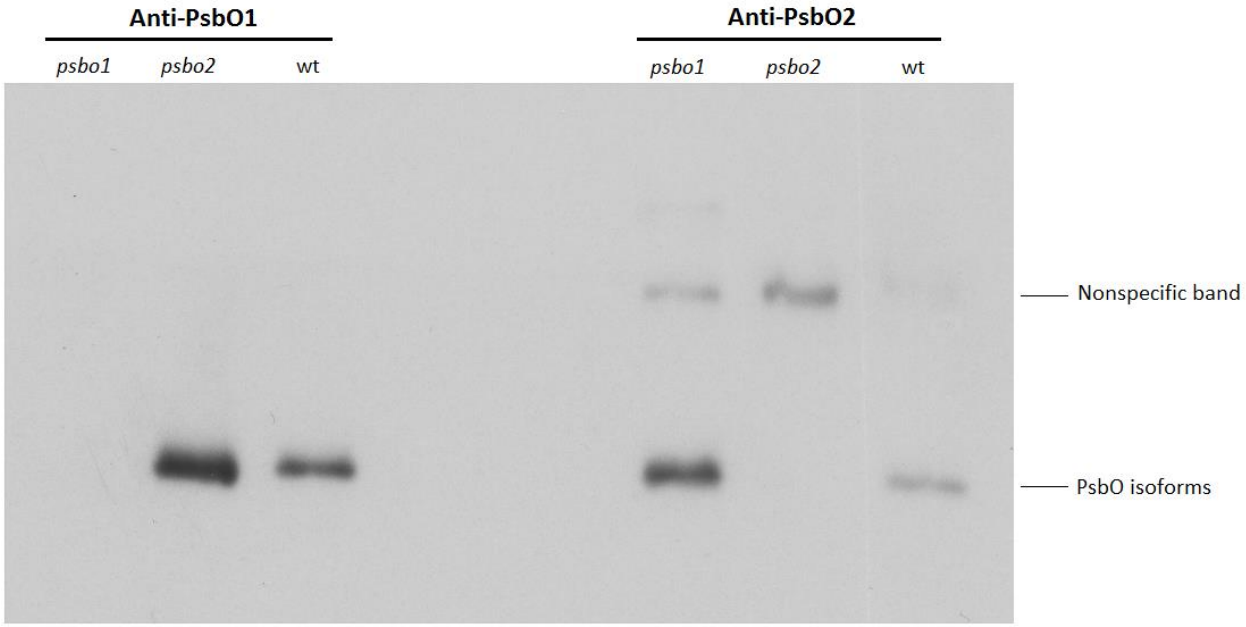

Figure 11. Western blot of thylakoids with anti-PsbO1 and anti-PsbO2 antibodies. Thylakoids were isolated from dark adapted *psbo1*, *psbo2* and wt plants. Membrane was cut to two pieces for incubation with antibodies and aligned again for blot development. Protein amount corresponds to 1 µg of Chl per lane.

The same WBs as mentioned above were used for protein quantification in mutants and wt. In Fig. 12 and Fig. 13, protein levels are plotted as relative amount of wild type (100 %) compared to mutants for each isoform separately. Wild type protein level (Fig. 12) of PsbO1 isoform (100 ± 6 %) was compared with *psbo2* mutant (170 ± 18 %), increase in *psbo2* was significant. Protein level of PsbO2 isoform (Fig. 13) was even more increased in *psbo2* mutant (353 ± 64 %) compared to wt level (100 ± 6 %) and was also significant.

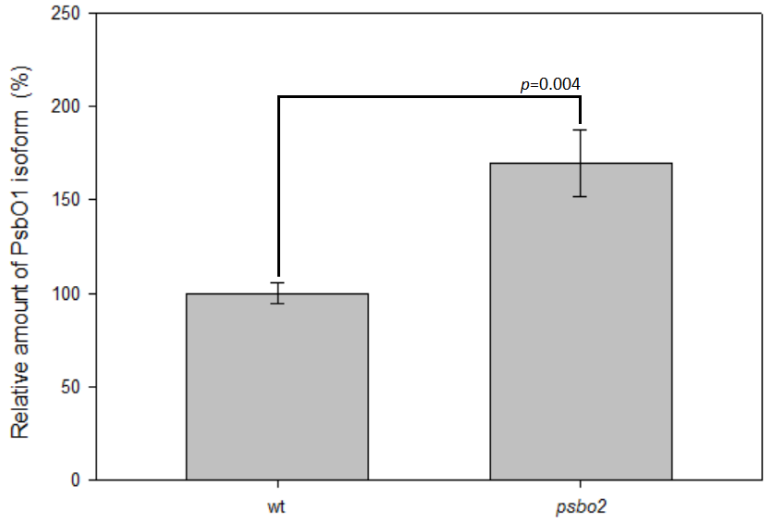

Figure 12. Relative levels of PsbO1 isoform in *psbo2* mutant in comparison with wild type. Means and SE are calculated from three biological replicates.

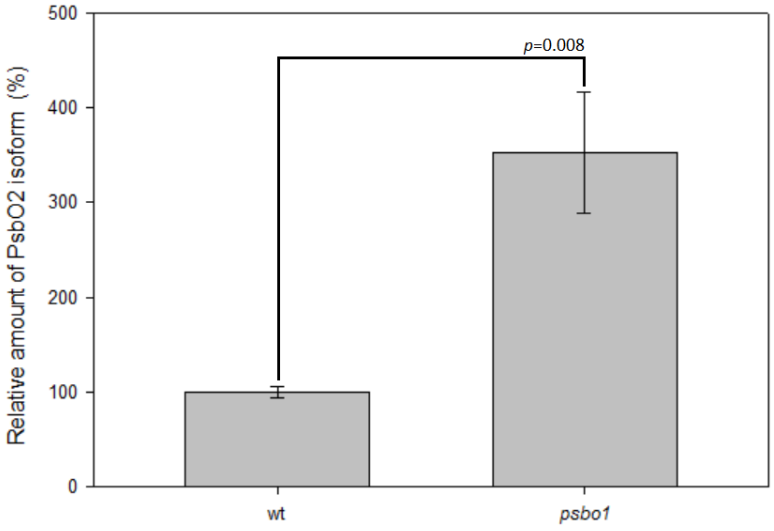

Figure 13. Relative levels of PsbO2 isoform in *psbo1* mutant in comparison with wild type. Means and SE are calculated from three biological replicates.

4.1.3.2 Antibody binding efficiency control

Prior to further experiments, antibodies binding efficiency control was done in order to find out whether densitometric quantification of WB bands is linearly dependent on amount of loaded proteins.

Logarithmic dilution series of TH isolated from *psbo1* and *psbo2* mutants were used for WB. Amounts of sample per lane were corresponding to 0.25, 0.5, 1 and 2 µg of chlorophyll (Fig. 14).

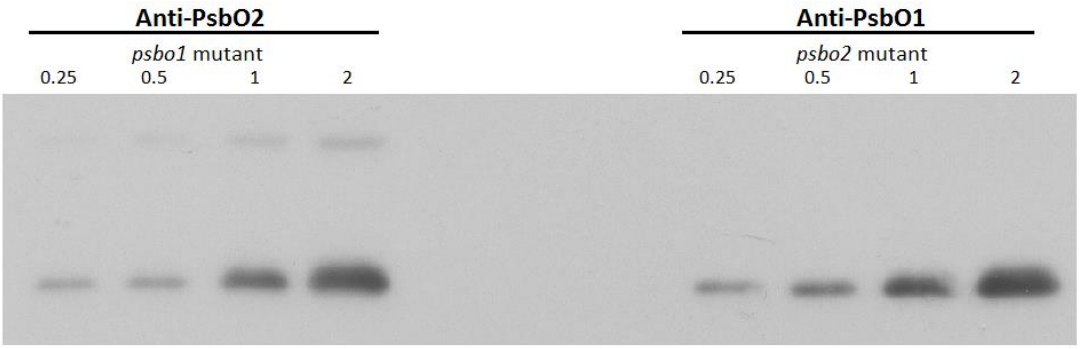

Figure 14. Western Blot with dilution series of thylakoids from *psbo1* and *psbo2* mutants. Amount of protein correspond to 0.25, 0.5 and 1 µg of chlorophyll per lane.

Bands on blots were densitometrically quantified and plotted against loaded amount of Chl to find out whether the staining is linear (Fig. 15). Staining was not completely linear, especially for the chlorophyll amount of 2 µg. Therefore, the exact numbers of WB quantifications should be considered in this context.

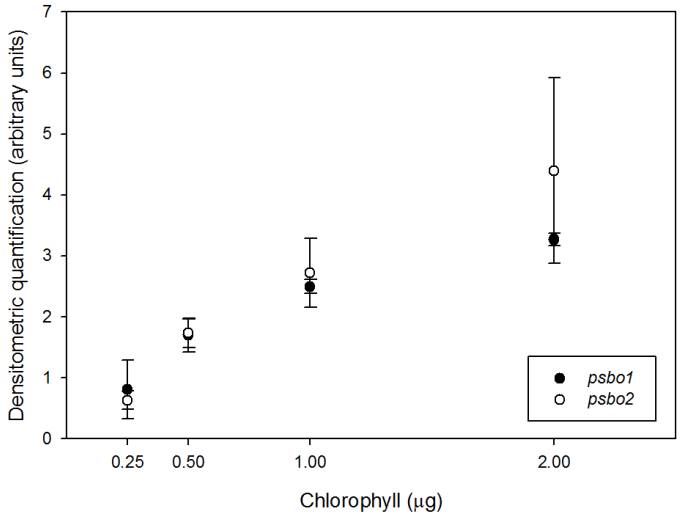

Figure 15. Binding efficiency of anti-PsbO1 and anti-PsbO2 antibodies. Densitometric quantification plotted against Chl amount (0.25, 0.5, 1 and 2 µg). Mean an SE are calculated from two biological replicates.

4.1.4 Cytochrome b_{559} determination in mutants and wt

Absorption spectroscopic measurement of integral photosystem II (PSII) protein cytochrome b_{559} (cyt b_{559}) was carried out in order to quantify PSII in TH of mutants and wt. Cyt b_{559} is present in all subpopulations of PSII in thylakoid membrane and has fixed 1:1 stoichiometry per reaction center (Puthiyaveetil et al., 2014). Mutant *psbo1* have lower amount, (1.86 ± 0.426) $\times 10^{-3}$, of cytochrome b_{559} per Chl than wt, (2.79 ± 0.686) $\times 10^{-3}$, and *psbo2*, (2.76 ± 0.175) $\times 10^{-3}$ (Fig. 16).

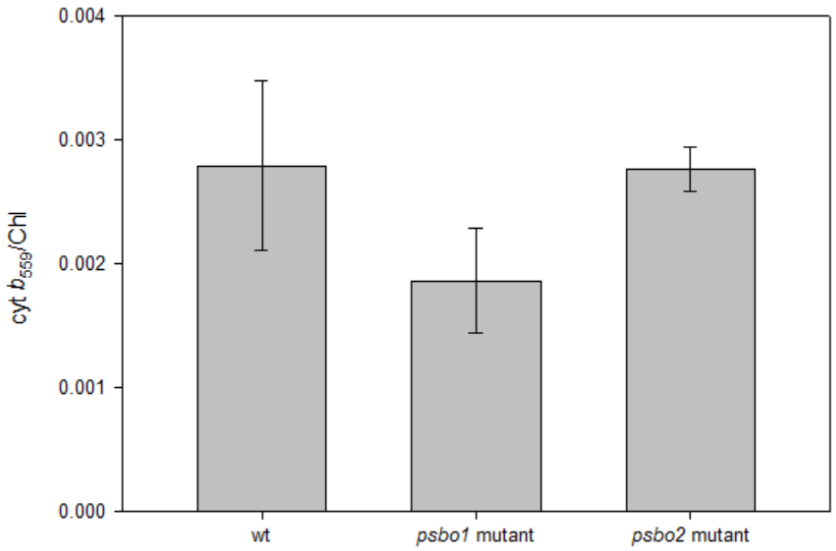

Figure 16. Amount of cytochrome b_{559} molecules per chlorophyll in thylakoids from wt and mutants. Mean and SE are calculated from two biological replicates.

4.1.5 Blue-Native PAGE of thylakoids of dark-adapted mutants and wt

Correct organization of thylakoid membrane protein complexes, PSII included, is essential for maintaining high rates of photosynthesis. Hence blue-native (BN) electrophoresis of solubilized thylakoid membranes from dark adapted wt and mutants was made to find out whether there are some alterations in levels of particular protein complexes in mutants. Isolated TH (50 μg of Chl per sample) were solubilized with α-dodecyl maltoside and loaded on the BN gel in two technical replicates each. BN showed changes in organization of protein complexes in *psbo1* mutant but no changes were observed in *psbo2* mutant compared to wt (Fig. 17). Decreased amount of *psbo1* PSII megacomplexes (MC), supercomplexes (SC) and band corresponding to PSII dimer, photosystem I (PSI) and ATPase was clearly visible.

Interestingly, it seems that chlorophyll amount is lower in lanes corresponding to *psbo1* mutant despite equal chlorophyll amount in starting material.

The most important step during sample preparation for BN electrophoresis is detergent solubilization of thylakoid membranes which is followed by centrifugation to remove unsolubilized material. The resulting pellet is usually very small but pellet in *psbo1* samples was much larger in comparison with wt and *psbo2*. Thus, probably some portion of chlorophyll-containing complexes was lost in the pellet during the preparation of *psbo1* sample. Initial experiments with Lugol's solution showed that starch and possibly some other compounds are present in the pellet.

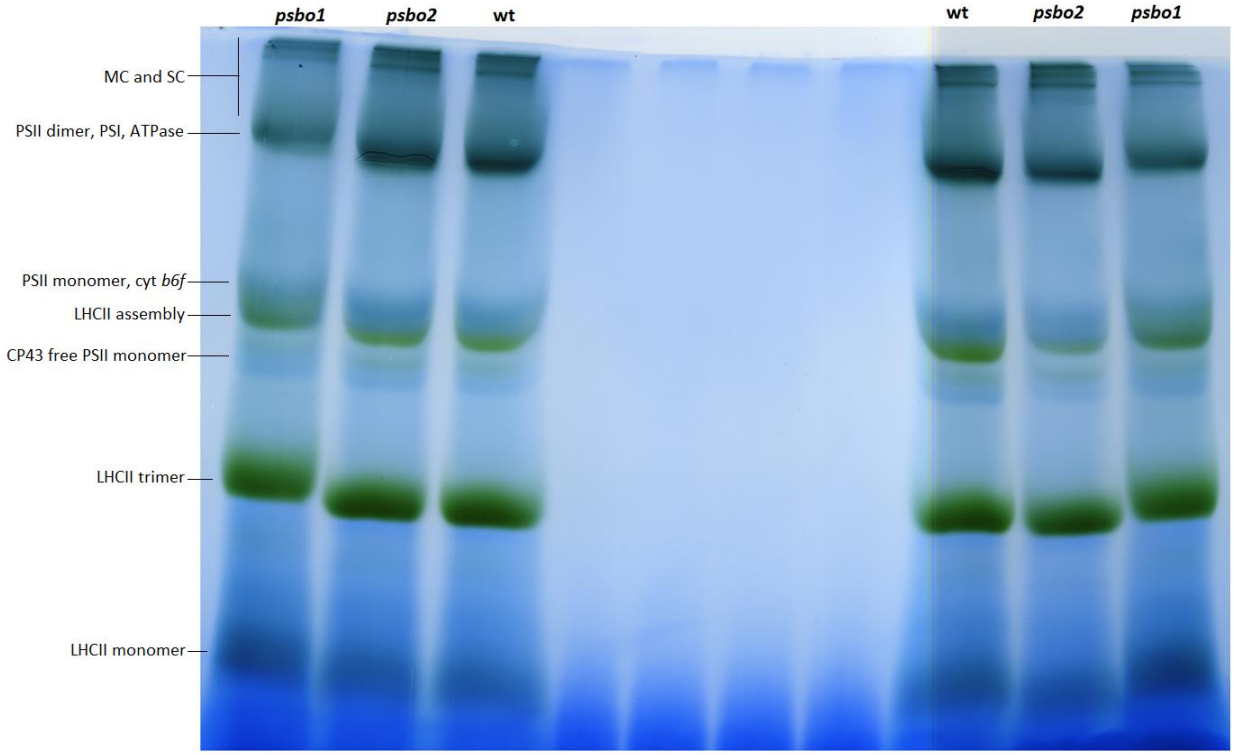

Figure 17. Blue-native PAGE analysis of thylakoid membranes of wt and mutants solubilized by 1 % α-dodecyl maltoside. MC – megacomplexes, SC – supercomplexes, PSII dimer – dimeric core of photosystem II, PSI – photosystem I, ATPase – thylakoid ATP synthase, PSII monomer – monomeric core of photosystem II, cyt *b6f* – cytochrome *b6f* complex, CP43 free PSII monomer - photosystem II monomeric core without CP43 subunit

4.1.6 Content of nonstructural saccharides in leaves

Pellet observed during blue-native PAGE sample preparation and Lugol's positive staining indicated possible alterations in saccharide metabolism in *psbo1* mutant. All three genotypes were further investigated for soluble saccharides and starch content by high-performance liquid chromatography (HPLC).

Total soluble saccharides content in *psbo1* was about two fold of that found in wt (Fig. 18). Mutant lacked detectable levels of monosaccharides such as glucose and fructose and had only traces of inositol. In wt, fructose and inositol were present in very low levels but glucose represented the absolute majority of soluble saccharides. Moreover, two unspecified oligosaccharides denoted as "unk1" and "unk2" were detected in *psbo1*. According to retention times, unk1 and unk2 were preliminarily determined as tetrasaccharide stachyose and trisaccharide raffinose, respectively. Unk1 was detected in *psbo1* only and represented 88 % of total soluble saccharides content. Although in significantly lower amount than in *psbo1*, Unk2 was detected also in wt (p = <0.001). Mutant *psbo2* did not show any alterations as compared to wt.

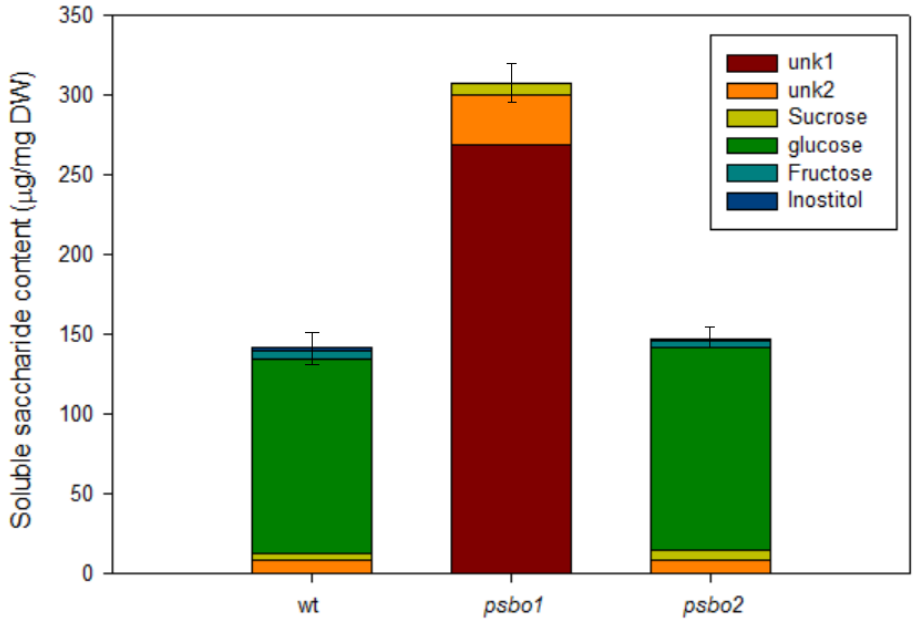

Figure 18. Soluble saccharides content in *psbo1*, *psbo2* and wt. Means and SE are calculated from six biological replicates.

Starch was determined as glucose equivalents after enzymatic digestion. Complementary to increased soluble saccharide levels, *psbo1* mutant showed decreased starch level (about 70 % of wt) while *psbo2* and wt did not show any alterations (Fig. 19). Interestingly, total content of nonstructural saccharides (soluble saccharides and starch) did not show any alterations in either genotype (Fig. 20).

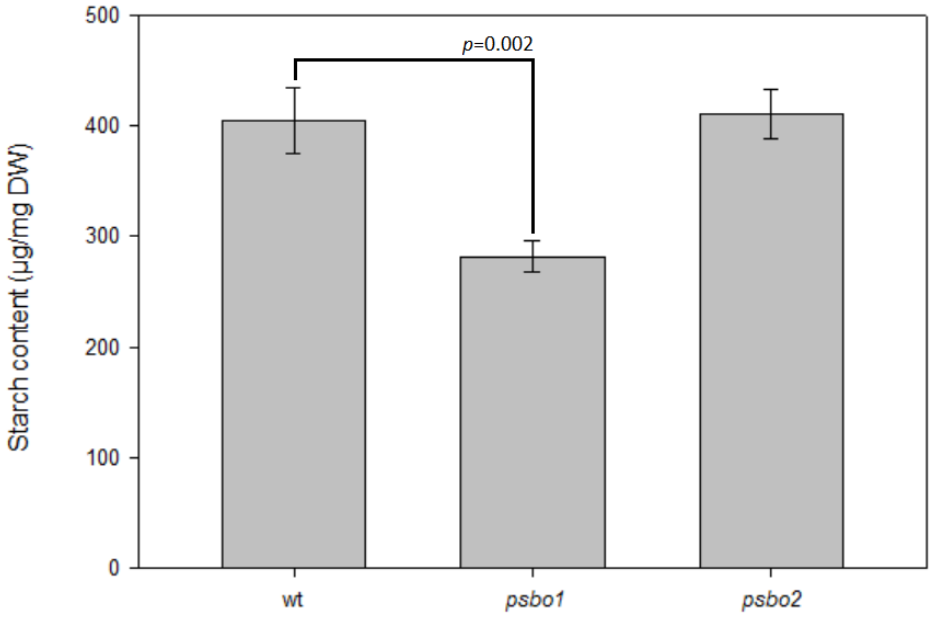

Figure 19. Starch content determination in glucose equivalents after enzymatic digestion. Mutant *psbo1* showed significant decrease in starch content while *psbo2* and wt did not show any alterations. Means and SE are calculated from six biological replicates.

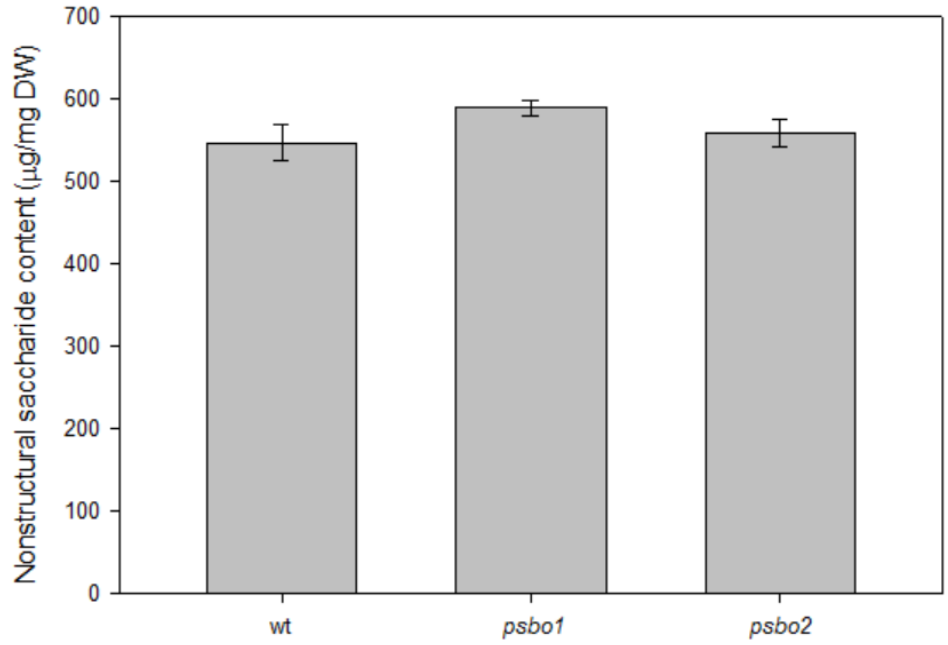

Figure 20. Total content of nonstructural saccharides (soluble saccharides and starch). Means and SE are calculated from six biological replicates.

4.1.7 Thylakoid structure of dark-adapted *psbo2* and wt plants

Structure of thylakoid membrane dynamically responds to light conditions (Herbstová et al., 2012), particularly grana core and grana margins can dramatically change their volume according to light. In order to test whether PsbO isoforms influence the thylakoid structure, amount of GC, GM and SL was measured in wt and *psbo2* plants.

Fractionation of thylakoid membranes of dark adapted wt and *psbo2* plants to GC, GM and SL was carried out with mild detergent digitonin. Mutants *psbo1* did not reach the desired amount of biomass for fractionation because of their impaired growth and could not be used for these experiments. The yield of particular thylakoid subfraction was measured as a percentage of chlorophyll that belongs to this fraction. According to Puthiyaveetil et al. (2014), percentage of chlorophyll corresponds directly to the percentage of membrane for each thylakoid subcompartment. Fraction yields showed no significant differences between *wt* and *psbo2* plants (Fig. 21).

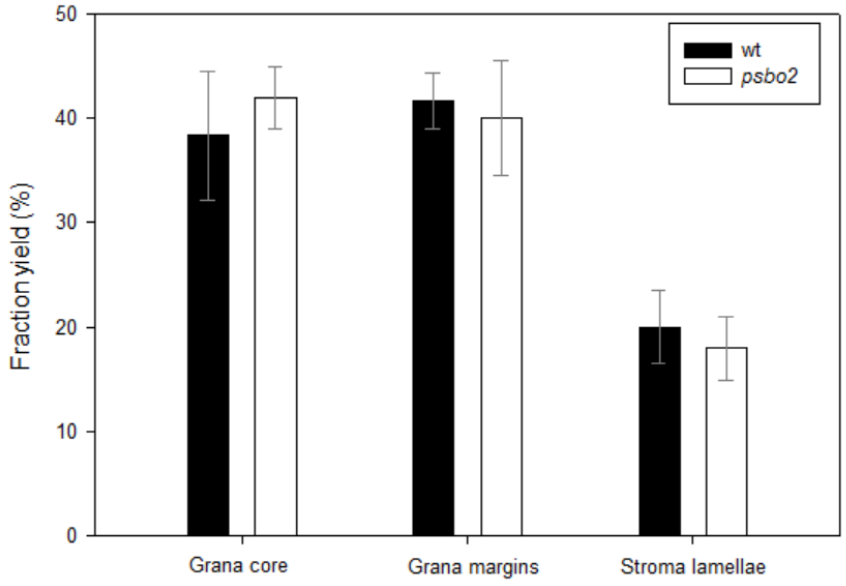

Figure 21. Fraction yields of wt and *psbo2* dark adapted plants. Means and SE are calculated from three biological replicates.

A good indicator of fraction quality is chlorophyll a/b ratio which should be around 2.4 for GC and more than 4.0 for SL. GM is GC and SL and should be around 3.5 but in general more than GC and less than SL (Puthiyaveetil et al., 2014 and personal communication with S. Puthiyaveetil). Our results (Tab. 16) show that the chlorophyll a/b ratio was quite high in GM (both in wt and *psbo2*), but still lower than in SL.

Table 16. Chlorophyll a/b ratios in fraction of dark adapted wt and *psbo2* plants. Numbers are means and SE from three biological replicates.

	Grana Core	Grana Margins	Stroma Lamellae
wt	**2.4** ± 0.06	**4.3** ± 0.52	**4.8** ± 0.44
psbo2	**2.5** ± 0.09	**4.1** ± 0.19	**4.3** ± 0.36

4.2 PsbO protein isoforms distribution depending on light conditions

Plants have to cope with ever changing environmental conditions including the fluctuations in light radiation causing stress. Response to light stress is realized on many levels from whole leaf to protein complexes in thylakoid membranes. In order to find out what happens with PsbO protein isoforms distribution during light stress, plants were treated with excess of light.

4.2.1 Blue-native PAGE of thylakoids of high light treated wt

Dark adapted wild type plants were treated with HL conditions (1200 μmol quanta·m^{-2}·s^{-1}) for 0 (dark adapted), 1 or 2 hours. F_v/F_m values were measured before and after treatment in order to control whether the plants were light stressed. Dark adapted plants were in good condition (F_v/F_m was 0.82 ± 0.004). Plants after treatment were significantly stressed, F_v/F_m value was 0.64 ± 0.029 and 0.66 ± 0.009 for 1 hour and 2 hours of HL respectively (means and standard errors were calculated from at least three independent measurements). TH were solubilized with the same method as described in chapter 4.1.5 and loaded on the BN gel in amount equal to 50 μg of Chl per lane in two technical replicates each.

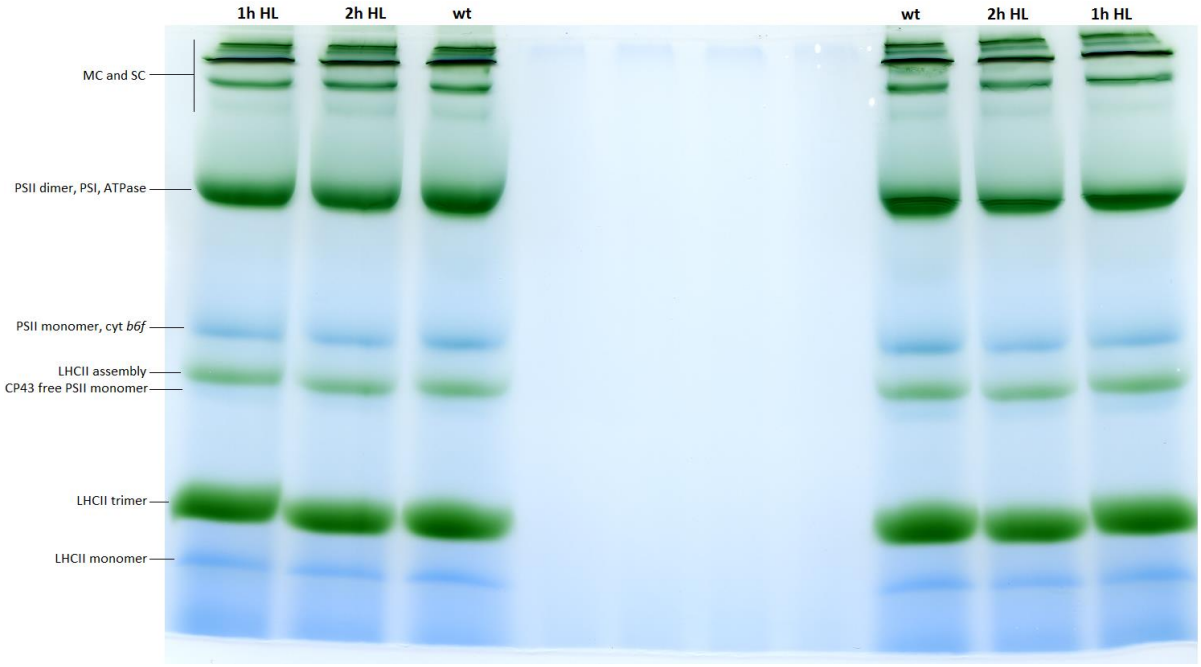

Figure 22. Blue-native PAGE analysis of thylakoid membranes of dark adapted and high light treated wt solubilized by 1 % α-dodecyl maltoside. Bands are denoted same as described under Fig. 17

Despite expected rapid changes in arrangement of PSII super and megacomplexes, no visible changes were observed (Fig. 22). High light treated and dark adapted samples seem to be very similar regarding the composition of photosynthetic complexes.

4.2.2 Quantification of D1 protein and cyt b_{559} in intact thylakoids

Protein D1, the core subunit of PSII, undergo rapid turnover because D1 is the main target of photodamage (Hundal et al., 1990). In order to see whether there are some changes in level of D1 and if there is any correlation with PsbO protein isoforms, WB with the same set of DA and HL treated TH was made. WB with anti-D1 antibody (Fig. 23) did not show any significant changes (Fig. 24) and it seems that even strong high light stress did not change the D1 protein level in short time scale of 1 or 2 hours.

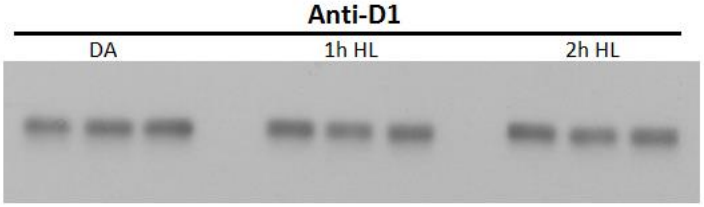

Figure 23. Quantification of D1 protein levels in dark adapted and high light treated thylakoids. Each triplicate corresponds to three biological replicates.

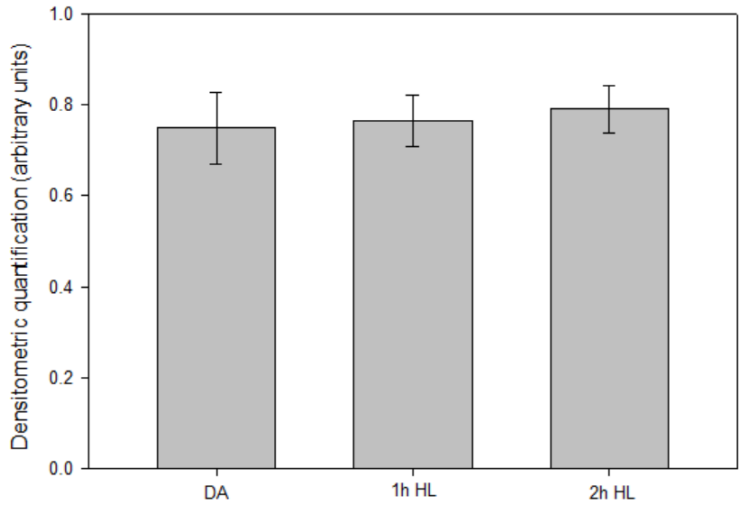

Figure 24. D1 protein levels in DA, 1h HL and 2h HL treated plants. Means and SE are calculated from three biological replicates

Measurement of cytochrome b_{559} confirmed the result obtained from D1 quantification and did not show any changes after the transfer to excess of light (Fig. 25).

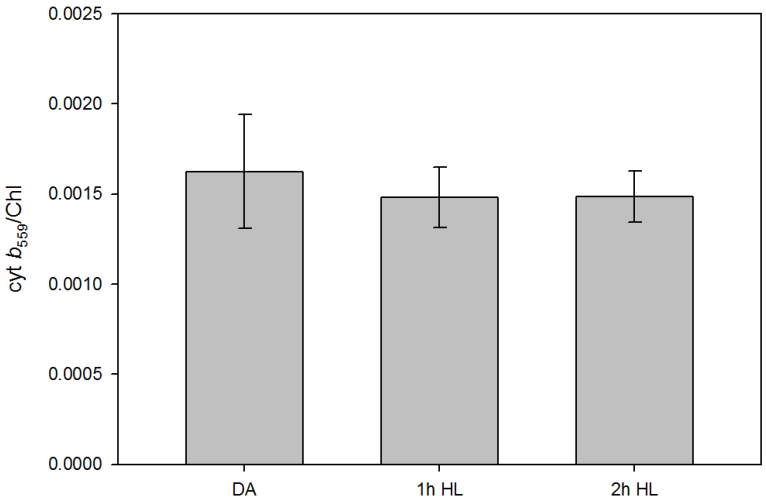

Figure 25. Spectroscopic determination of cytochrome b_{559} in intact thylakoids. Means and SE are calculated from three biological replicates.

4.2.3 Fractionation of thylakoid membranes of high light treated wt plants

Under excess of light, thylakoid membranes undergo changes in their organization in order to be able to efficiently repair photodamaged PSII and maintain high rates of photosynthesis. This change in thylakoid membranes organization consists of increase

in yield of GM and complementary decrease in yield of GC (Puthiyaveetil et al., 2014) without changes in yield of SL fraction.

4.2.3.1 Fractionation yields of high light treated plants and comparison to dark adapted plants

Dark adapted plants were treated with the same illumination as plants for Blue-Native PAGE (1200 μmol quanta·m^{-2}·s^{-1} for 0, 1 or 2 hours). F_v/F_m spectra were measured before and after treatment. Dark adapted plants showed slightly lower values (0.74 ± 0.034) than plants used for BN-PAGE but they still were in good condition. HL treated plants reached values (0.53 ± 0.003 and 0.57 ± 0.006) which is again a bit lower than values for plants used for BN-PAGE, but it corresponds to lower starting values of dark adapted plants. Means and standard errors were calculated from three independent measurements. Fraction yields did not show statistically significant differences between dark adapted and high light treated plants (Fig. 26) but decreasing trend was clearly visible in GC fraction, while increasing trend was visible in GM fraction. Yields for 1 hour of high light treated plants were following: GC 37 ± 3 %, GM 44 ± 3 %, SL 23 ± 0.3 % and for 2 hours treated: GC 33 ± 2 %, GM 47 ± 3 %, SL 20 ± 3 %.

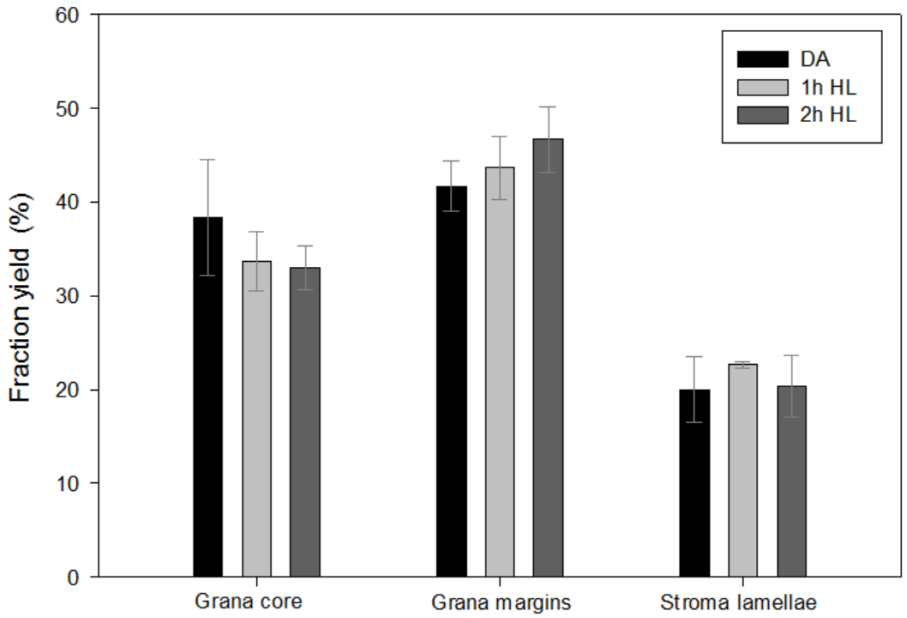

Figure 26. Yields of thylakoid fractions of dark adapted (DA) wt plants and wt plants treated with HL for 1 and 2 h Means and SE are calculated from three biological replicates.

Chlorophyll a/b ratio was measured for fraction quality control as described in chapter 4.1.7. All fractions of HL treated plants showed good ratios according to protocol (Tab. 17). Chlorophyll a/b ratios of HL fractions are compared with DA fractions.

Table 17. Chlorophyll a/b ratios in fraction of dark adapted wt and high light treated wt plants. Numbers are means and SE from three biological replicates.

	Grana Core	Grana Margins	Stroma Lamellae
DA	**2.4** ± 0.06	**4.3** ± 0.52	**4.8** ± 0.44
1h HL	**2.4** ± 0	**3.5** ± 0.15	**4.1** ± 0.15
2h HL	**2.5** ± 0.03	**3.4** ± 0.1	**4.0** ± 0.06

4.2.3.2 Lumenal fraction in comparison with dark adapted and high light treated plants

Thylakoid lumen is continuous compartment enclosed by thylakoid membrane. Lumenal proteome contains at least 80 proteins (Järvi et al., 2013) and most of them still have unknown function. It has been reported (Kieselbach et al., 1998) that lumen also contains relatively high amount of PsbO protein in spinach.

Lumenal fractions from dark adapted and high light treated plants were isolated in order to make investigation of alterations in PsbO isoforms amounts after the transition from dark to the excess of light. Plants were treated in the same way as described in chapter 4.2.1. F_v/F_m spectra were measured before and after treatment. Dark adapted plants showed good condition (0.82 ± 0.006) and high light treated plants dropped to 0.69 ± 0.012 and 0.65 ± 0.003 after 1 hour and 2 hours of HL respectively. Determination of total protein amount was done in isolated lumenal fractions by Bradford protein assay (Fig. 27). Interestingly, after the transition to HL significant decrease of total lumenal protein was observed.

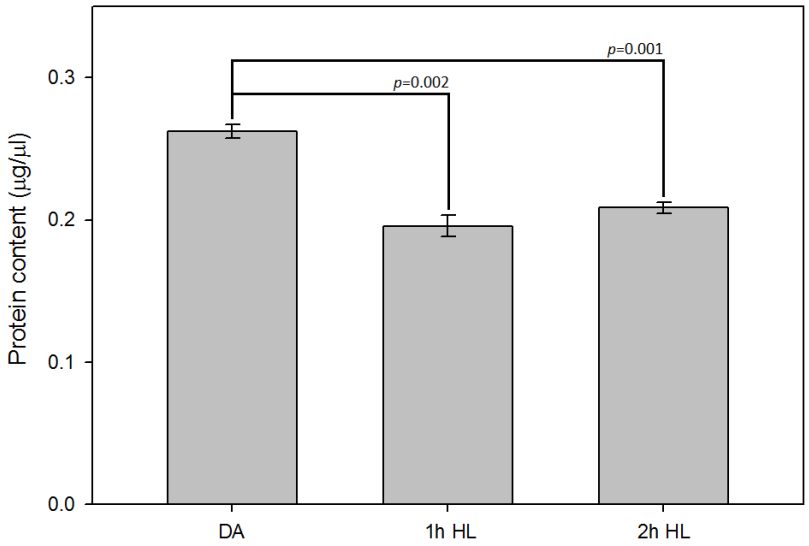

Figure 27. Concentration of proteints in isolated lumen. Dark adapted (DA) wt plants and wt plants treated with HL for 1 and 2 h. Determination by Bradford protein assay. Means and SE are calculated from three biological replicates.

4.2.4 Immunodetection of PsbO protein isoforms

4.2.4.1 PsbO protein isoforms distribution in dark adapted and high light treated plants

Fractions were used for WB in two different orders of loading. Firstly, all fraction from each fractionation (thylakoids included) were loaded on the gel in two technical replicates side by side in order to detect both isoforms from each fractionation. Secondly, different order of loading was used in order to observe time changes in particular fraction after the transfer to HL. Thus each fraction and TH were loaded on the gel separately, three biological replicates of each treatment (DA, 1h HL, 2h HL). Therefore, each sample was densitometrically quantified twice, which allowed to normalize the data for further investigation.

Western blots with TH and particular fractions (GC, GM, SL) showed heterogenic distribution of PsbO protein isoforms within thylakoid membrane. Since TH is a mixture of all fractions and usually showed similar levels as GC, statistics were made within the fractions only.

Statistics showed significantly lower levels of both isoforms per Chl in each light treatment in GM compared to GC (Fig. 28). Both isoforms showed highest levels in GC while lowest levels in GM fraction.

When relative levels of PsbO1 and PsbO2 isoform were compared to GC as 100 % for each (Fig. 29) statistics showed significantly higher levels of PsbO1 than PsbO2 in GM isolated from DA and 1h HL plants (Fig. 29A and B). This difference was not observed after 2h HL (Fig. 29C). Cannot be said if there is low level of PsbO2 in GM or high level of PsbO2 in GC. Relatively, difference between GC – GM levels is more pronounced in case of PsbO2 isoform. After transfer from dark to HL, significant difference between isoform levels was observed in SL fraction, which may be due to bigger error bars in DA for both isoforms in SL.

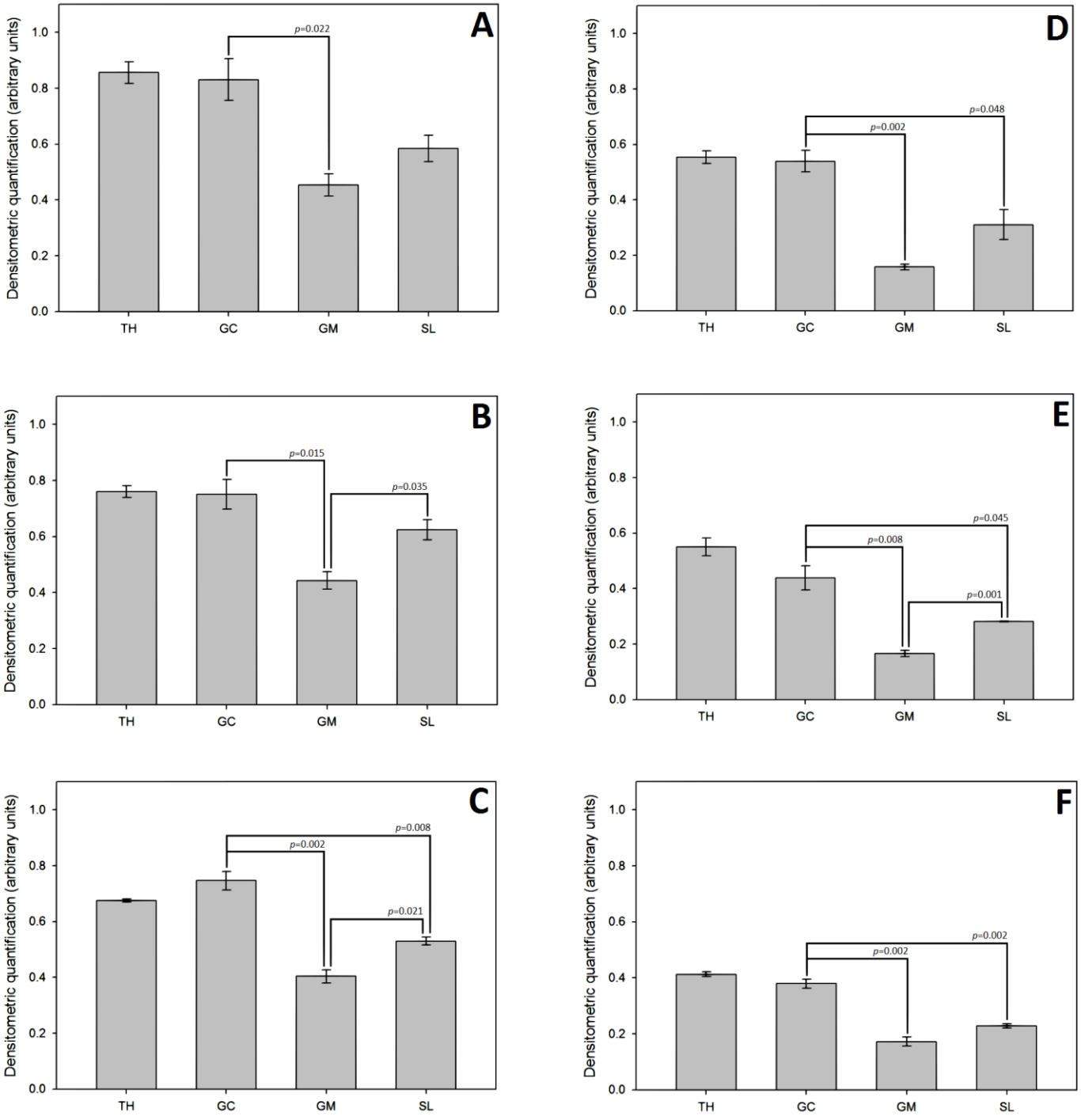

Figure 28. Quantification of both isoforms in dark adapted and high light treated fraction including thylakoids by western blotting. Quantification of PsbO1 isoform represent graphs A, B and C for DA, 1h HL and 2 h HL respectively. Quantification of PsbO2 isoform represents graphs D, E and F for DA, 1h HL and 2 h HL respectively.

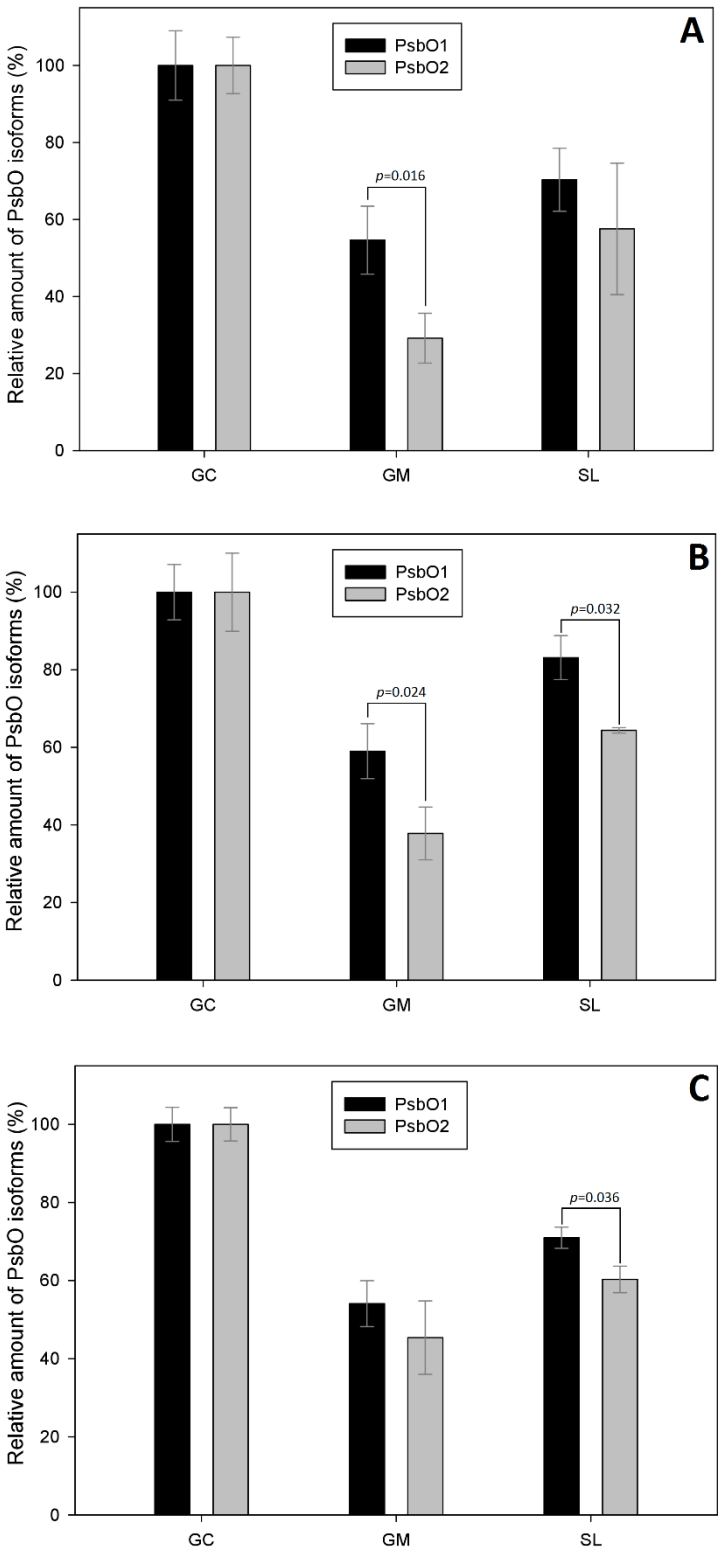

Figure 29. Relative levels of PsbO isoforms based on GC as 100 %. Graphs A, B and C represent DA, 1h HL and 2h HL respectively

In order to see what happens in fractions on time scale of 0 – 2 h of light stress, data were plotted for each isoform separately to clearly observe changes in protein levels in particular isoform (Fig. 30).

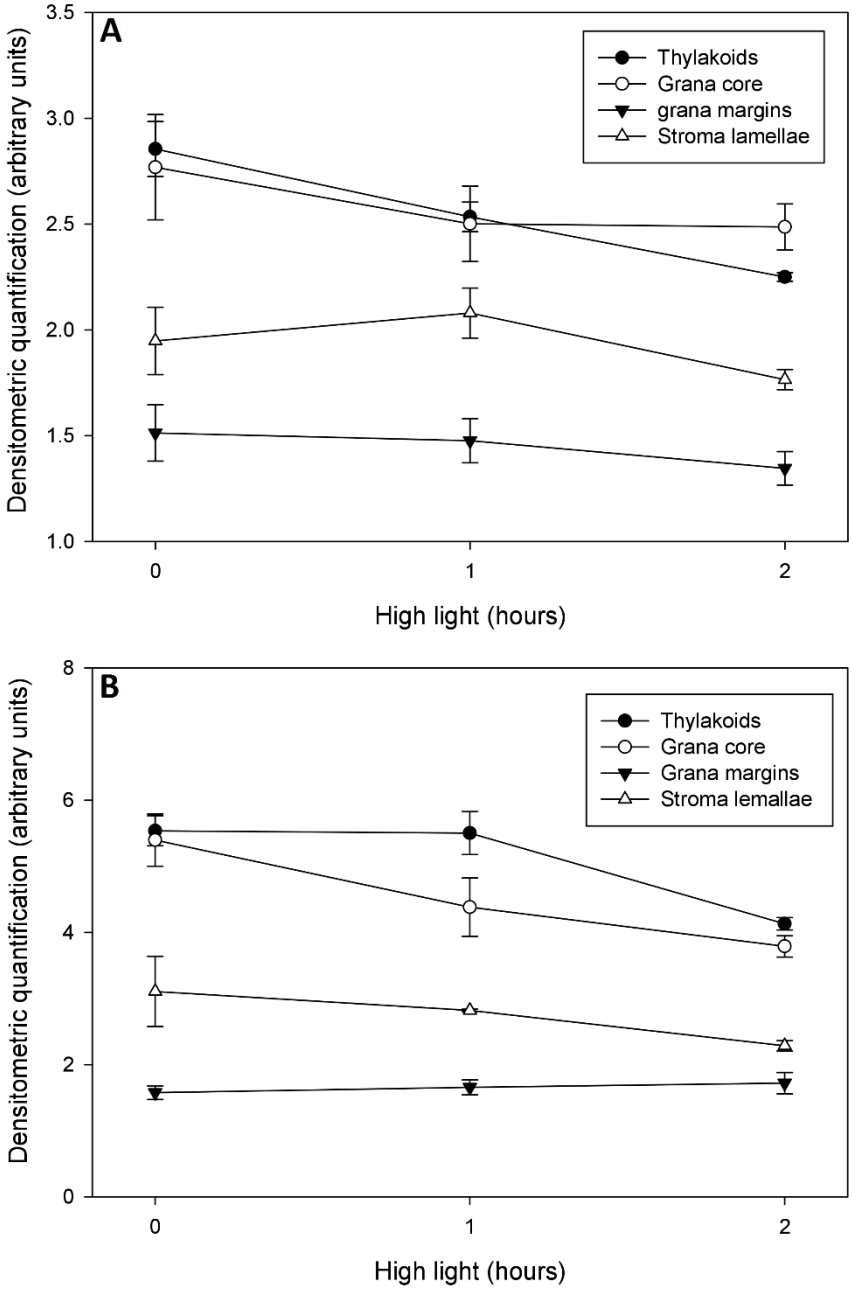

Figure 30. Timescale of DA, 1h and 2h HL treatment. **A** represents PsbO1 isoform, **B** represents PsbO2 isoform.

Decrease of PsbO1 in TH and GC is not significant (Fig. 30A), GM and SL fraction seems to be still with only little changes. Situation is different in case of PsbO2 isoform (Fig. 30B), observed decrease in TH and GC is significant between 0 and 2 h HL with *p*-values $p = 0.009$ and $p = 0.037$ for TH and GC respectively. GM and SL fraction did not show changes.

Total PsbO isoforms amount in TH was calculated in order to observe whether there are any lost during fractionation. Calculation was following: densitometric quantification which corresponds to 1 µg of Chl for every sample was multiplied by total Chl amount in particular fraction and TH. Theoretically, without any loss, GC + GM + SL should give the same amount as TH used for fractionation. Calculation showed that high amounts of PsbO protein are lost during fractionation (Fig. 31).

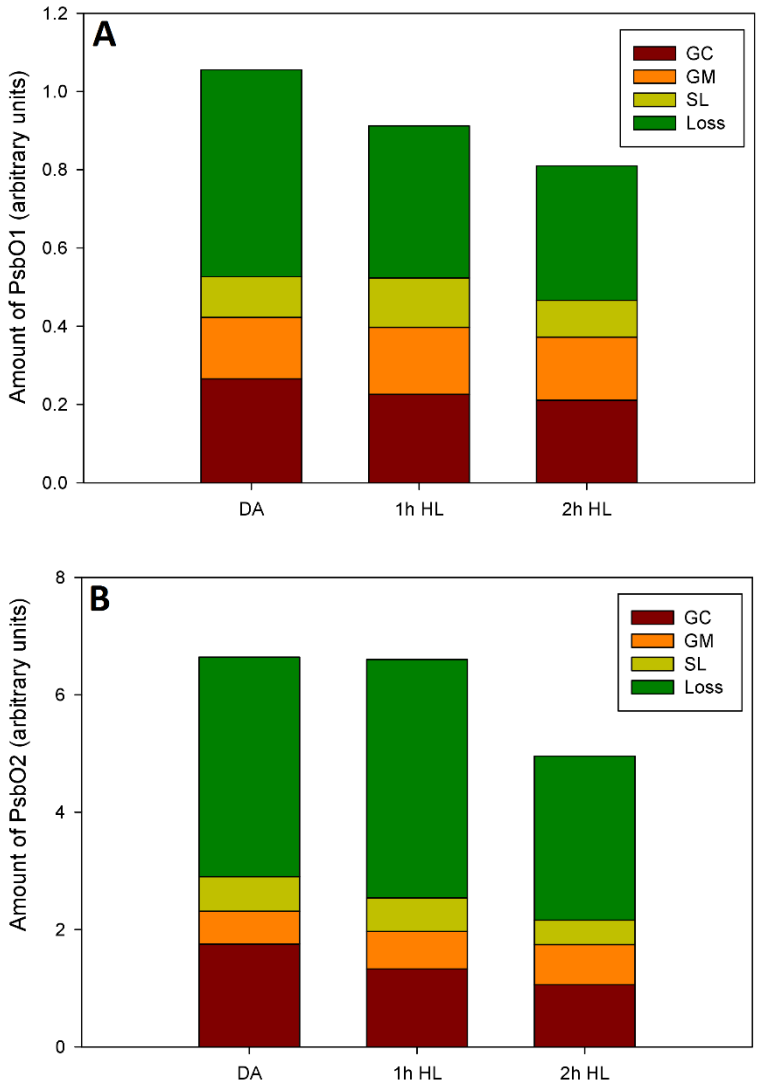

Figure 31. Total PsbO protein amount in fractions including loss during fractionation. **A** represents PsbO1 isoform, **B** represents PsbO2 isoform. Graphs have different scaling on Y axis.

Both graphs (Fig. 31A and B) show a trend in moving PsbO from GC to GM which correlates with decreasing yield of GC fraction and increasing yield of GM fraction after transfer to light stress (Fig. 26). Loss of PsbO1 is decreasing during 1 h and 2 h HL

but decrease is not significant, similar trend was observed also for PsbO2 but only in 2h HL. Compared to total protein amount in TH, the loss is relatively higher in case of PsbO2 isoform.

4.2.4.2 Lumenal fraction

Lumenal fraction showed some interesting results regarding to PsbO protein isoforms amount (Fig. 32). In high light significant increase of PsbO1 and PsbO2 occurs. On the blots it is clearly visible that two bands of desired size are detected. The lower band corresponding to smaller size of detected protein is thicker and more intense in both isoforms. Dark adapted samples of PsbO1 showed also two bands while samples of PsbO2 showed only the lower band probably due to overall low amount of PsbO2 protein.

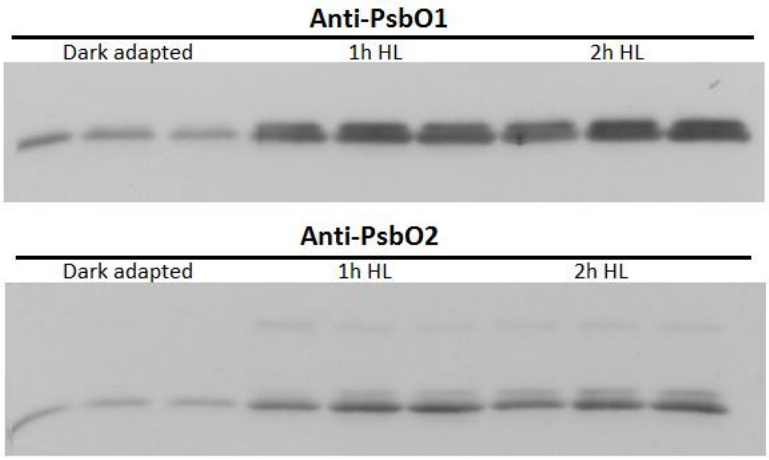

Figure 32. Lumenal fraction of dark adapted and high light treated wt plants. Each treatment is showed in triplicate which corresponds to three biological replicates.

The blot detected with anti-PsbO2 antibody also showed third band visible in the upper part of the picture, this corresponds to the nonspecific band mentioned before.

Total increase of PsbO protein isoforms is showed in Fig. 33. Increase of PsbO1 (Fig. 33A) isoform in lumen was 179 ± 7 % and 215 ± 7 % for 1 and 2 hours of high light respectively, numbers are compared to dark adapted which correspond to 100 %. Increase of PsbO2 isoform was even more pronounced (Fig. 33B) with following numbers: 232 ± 13 % and 287 ± 10 % 1 and 2 hours of high light respectively, compared to dark adapted as for PsbO1. Increase of PsbO isoforms in lumen is plotted with TH where decrease in levels of isoforms was observed.

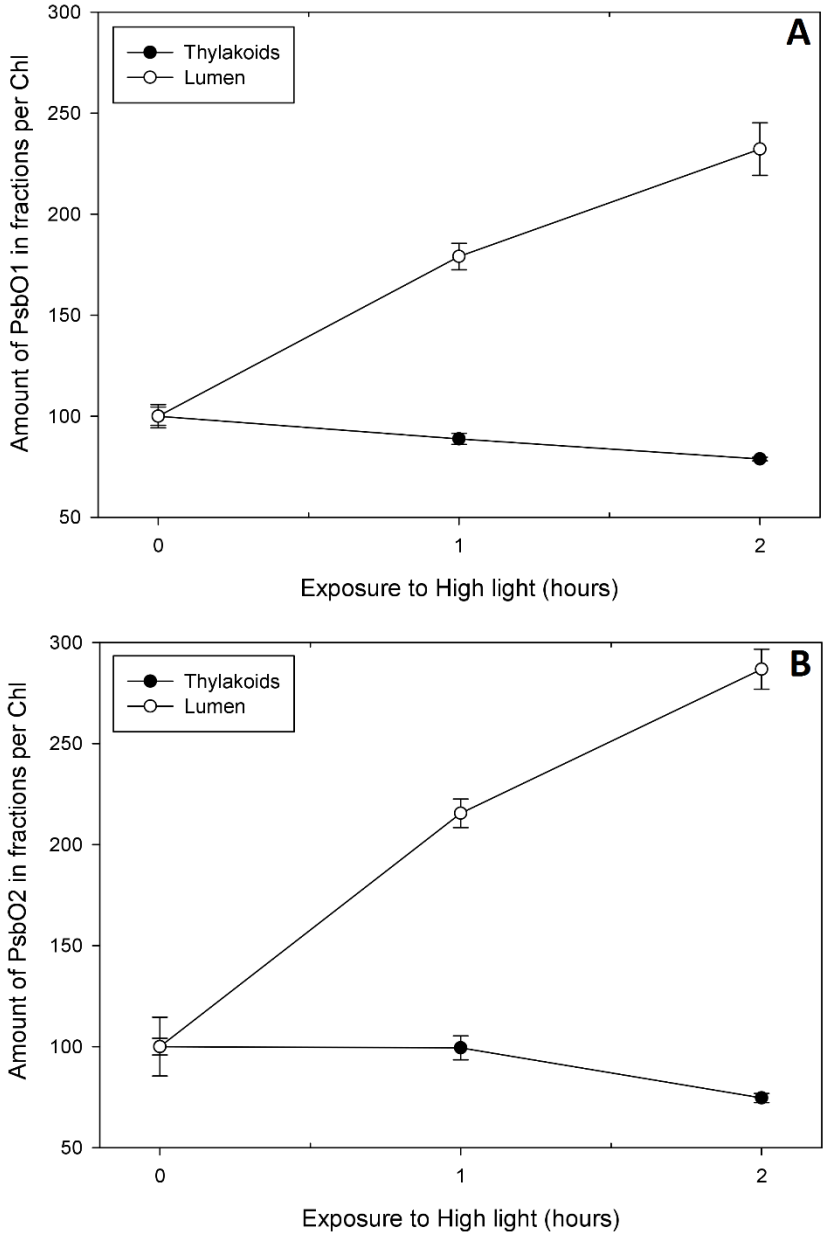

Figure 33. Relative increase in PsbO isoform levels in lumen during HL. Compared with decrease in thylakoids. Means and SE are calculated from three biological replicates.

WB for quality control of lumenal fraction was made, samples containing lumen were loaded on the gel along with GC fraction and detected with D1 antibody. This served as negative control to find out whether the lumen is contaminated with thylakoid membranes. No bands (Fig. 34) were detected in lumen containing samples, GC showed strong band corresponding to D1 protein.

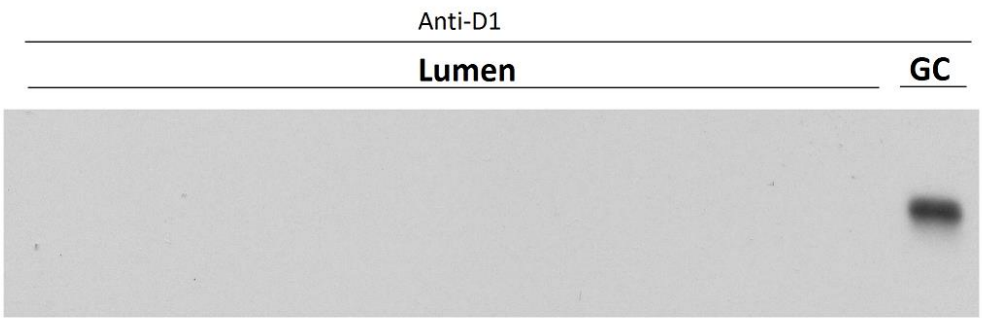

Figure 34. WB with anti-D1 antibody. Negative control of purity of luminal fraction, as positive GC fraction was loaded on the gel.

5 Discussion

Arabidopsis thaliana expresses two isoforms of *psbO* gene, PsbO1 and PsbO2. In order to find out particular role of isoforms in maintaining of photosynthesis and acclimation to short light stress, we made extensive biochemical investigation.

5.1 Characterization of *psbo1* and *psbo2* mutant plants

T-DNA mutants *psbo1* and *psbo2* and wt Col-0 were grown in growing chambers under GL conditions (100 μmol quanta·m^{-2}·s^{-1}). Plants *psbo1* showed pronounced phenotype with pale green leaves and retarded growth as compared to wt (Fig. 8 and 9), corresponding to previous observations (Murakami et al., 2002; Lundin et al., 2007a; Allahverdiyeva et al., 2009). Mutant *psbo1* also exhibited significantly lower (about half of wt) DW/FW ratio of leaf mass (Fig. 10). This characteristic highlights the importance of presence of PsbO1 isoform. In contrast, RNAi induced decrease of PsbOs even to 25 % of wt did not alter DW/FW ratio (Dwyer et al., 2012). On the other hand, plants *psbo2* did not show any visible change in phenotype as compared to wt under our cultivation conditions (Fig. 8 and 9). This observation is in line with Allahverdiyeva et al. (2009) and Suorsa et al. (2016), but differs from that of Lundin et al. (2007). Lundin and coworkers observed *psbo2* plants that grew slower than wt and showed dark green, more elongated leaves with bent edges. The difference may be caused by different cultivation, since their plants were grown hydroponically. In our conditions, statistics showed significantly lower (by 12.5 %) DW/FW ratio also for *psbo2* (Fig. 10), although the difference was much smaller as compared to *psbo1*.

Biochemical investigation of mutants consisted of blue-native PAGE of thylakoids, digitonin fractionation of thylakoid membranes, immunodetection of PsbO isoforms on WB, measurement of nonstructural saccharides content and measurement of cytochrome b_{559} level. Plants *psbo1* showed lower levels of megacomplexes (MC) and supercomplexes (SC) and photosystem II (PSII) dimers as compared to wt (Fig. 17). It is likely that some portion of thylakoid membrane complexes was lost in a pellet, observed after solubilization, that was bigger compared to *psbo2* and wt. Even so, lower levels of PSII subpopulations corresponded to lower levels of cyt b_{559} in this mutant (Fig. 16). Immunodetection on WB with *psbo1* showed significantly increased levels of PsbO2 isoform in the mutant (about 350 % of wt PsbO2 level; Fig. 13). We could not directly compare stoichiometry between isoforms in wt because of use

of isoform specific antibodies, therefore we are not able to claim what was the ratio between isoforms in our plants. Thus, we cannot state whether amount of PsbO2 in *psbo1* mutant is lower or higher than total PsbO in wt. The increase still could not compensate for lacking PsbO1 isoform, because in wt, PsbO2 level is only about 10–20 % of total PsbO (Murakami et al., 2005; Lundin et al., 2007 respectively) although Dwyer et al. (2012) observed 40 % of PsbO2. Thus in our cultivation conditions the amount of PsbO2 in *psbo1* mutant can be theoretically between 35–140 % of total PsbO in wt.

During characterization of *psbo1* mutant, we observed unusually big pellet in the sample after α-DM solubilization before BN-PAGE. Pellet showed positive reaction with Lugol's solution. This indicated altered starch content/metabolism. Therefore, measurement of nonstructural saccharides content using HPLC was done. Most interesting results gave measurement of content of soluble saccharides in *psbo1* (Fig. 18). At the end of night, *psbo1* mutant showed undetectable amount of glucose, which is the major soluble saccharide in wt. This is a very bizarre observation in the context of genetic studies which revealed hexokinase (HXK) as a conserved glucose sensor which acts as a core component in plant sugar sensing and signaling (reviewed in Rolland et al., 2006). In general, plant should not be able to survive without glucose. Although *psbo1* showed distinct phenotype, plants were able to reach the mature size of wt and *psbo2*, but after 12 weeks of growth in contrast to 7-8 weeks for wt and *psbo2* (not shown). One explanation may be that *psbo1* has impaired starch degradation, therefore this mutant is able to grow only during the day. This could explain the observation of the major soluble saccharide unk1 in *psbo1* assuming that it is not the preliminary determined tetrasaccharide stachyose, but maltotriose. Maltotriose is intermediate of starch degradation which accumulates during the night in *dpe1* plants with inactivated disproportionating enzyme (DPE1). DPE1 prefers maltotriose as substrate and produces glucose (Stettler et al., 2009). This explanation would correspond with our data, since samples were prepared from dark adapted (DA) plants. This assumption still needs further investigations, particularly measurement of sugar content during light period.

Conversely to higher soluble saccharides content, *psbo1* revealed lower amount of starch as compared to wt (Fig. 19). Apparently, this result is in discrepancy with initial observation of big pellet and Lugol's staining. There are two explanations, either the pellet did not consist only of starch granules, or alternatively starch granules could resist enzymatic degradation during sample preparation. The latter mentioned would correspond to Stettler et al. (2009), who observed enlarged starch granules in *dpe1* mutant. It is need to note that *dpe1* showed same

phenotype as wt. Clearly, *psbo1* has impaired saccharide metabolism, however, the interconnection between the missing PsbO1 isoform and metabolism of saccharides remains unclear.

DW/FW ratio and amount of PsbO were the only observed characteristics in which *psbo2* differed from wt. WB showed significantly increased level of PsbO1 as compared to wt. In wt, PsbO1 is the major isoform, reported to represent 60–90 % of total PsbO. Mutant *psbo2* contained about 170 % of PsbO1 compared to wt (Fig. 12), which is in line with previous observation (Lundin et al., 2007a). The increase is most likely caused by the absence of PsbO2 and therefore unbalanced expression. Lundin and coworkers (2008) suggested that PsbO1 isoform is less efficient in PSII repair cycle compared to PsbO2. They also reported higher levels of PSII-LHCII in *psbo2*. Thus, more PSII with slower repair cycle could be able to compensate this deficiency Conversely, regarding PSII complexes, our results differ from that of Lundin (Fig 17). We observed same sets of PSII complexes in *psbo2* and wt, moreover also levels of cyt b_{559} were same (Fig. 16). Other investigated characteristics such as nonstructural saccharides content and digitonin fractionation of *psbo2* thylakoid membranes did not show any alterations in comparison with wt.

5.2 PsbO isoforms during high light stress

Lundin et al. (2007) and Allahverdiyeva et al. (2009) proposed that PsbO2 is involved in PSII repair cycle. To test this hypothesis, plants were exposed to excess of light.

Although it is widely accepted that PSII supercomplexes undergo rapid rearrangement under excess of light (Fork and Satoh, 1986; Allen and Forsberg, 2001), we did not observe any significant changes in composition of PSII subpopulations after exposure to short high light (HL) stress (Fig. 22). Plants exhibited the same sets of MC, SC and PSII dimers for DA and HL exposed plants, this observation is in line with Fristedt et al. (2009), who exposed plants to HL for longer period and lower intensity (900 µmol photons m^{-2} s^{-1} for 3 hours). In our experiments, also D1 protein (Fig. 24), integral subunit of PSII core complex and main target of photodamage, and cyt b_{559} (Fig. 25) showed stable levels during HL. Cyt b_{559} has fixed 1:1 stoichiometry per reaction center and is present in all PSII subpopulations.

Puthiyaveetil et al. (2014) showed that thylakoids undergo architectural switches during HL. Yield of grana core (GC) decreased while yield of grana margins (GM) increased

(Puthiyaveetil et al., 2014). We had lower yield of GC fraction from DA plants as compared to cited work and the HL switch was not statistically significant but a similar trend was clearly visible (Fig. 26).

Immunodetection of PsbO isoforms in isolated wt thylakoid subcompartments revealed heterogenic distribution of the isoforms. Both isoforms were localized in highest amounts in GC fraction (the amount per Chl was similar to whole thylakoids). On the other hand, GM exhibited lowest amounts of both PsbO isoforms per Chl. The amount of both PsbO isoforms in stroma lamellae (SL) was between that of GC and GM (Fig. 28). When comparing PsbO1 and PsbO2 isoform, we observed different GC:GM ratios. In GM, PsbO1 showed 55 % of that in GC while PsbO2 had only 29 % of GC level. Since PsbO is extrinsic subunit of PSII, its heterogenic distribution would be related to unequal distribution of PSII (containing the respective isoforms) in thylakoid subcompartments (Herbstová et al., 2012; Puthiyaveetil et al., 2014). Puthiyaveetil et al. (2014) reported that in SL is lower level of PSII than in GM in DA. In context of our results it means that either free PsbO is localized in SL or PSII without PsbO are localized in GM. The latter mentioned is more likely, as it was reported that during PSII repair cycle PsbO is released to lumen to allow efficient D1 replacement (Hundal et al., 1990).

PsbO levels in fractions did not show any big changes after exposure to HL (Fig. 30). We observed decrease of PsbO per Chl in GC which was significant just in case of PsbO2 after 2 h HL (Fig. 30B). Relative to GC levels, PsbO2 showed increase in GM (Fig. 29A-C), in DA conditions PsbO2 was significantly lower than PsbO1, while after 2 h of HL this difference was not observed. If the PSII with PsbO2 is more mobile and is able to rapidly reach GM, where D1 is degraded (Puthiyaveetil et al., 2014), these results may support the suggested role of PsbO2 in repair cycle.

It was reported that extrinsic subunits PsbO, PsbP and PsbQ along with mobile carrier PC are the most abundant proteins found in spinach thylakoid lumen (Kieselbach et al., 1998). Their findings suggest that at least some part of PsbO population is unbound in lumen. Ettinger and Theg (1991) reported only low amounts of PsbO in pea lumen and almost undetectable amounts in spinach lumen. We detected a small amount of both PsbO isoforms in lumen isolated from DA plants (Fig. 32). However, the situation dramatically changed after exposure to HL. Continuous increase up to 200 %–300 % was observed during 2 h of HL (Fig. 33). Increase was more remarkable in case of PsbO2 isoform (Fig. 33B).

Analysis of lumen brought another interesting result, for both isoforms, two bands of similar molecular weight were detected (Fig. 32). Band corresponding to lower molecular weight was more intense for both PsbO1 and PsbO2. In the DA samples it is clearly visible that the majority of detected protein corresponds to smaller molecular weight. *In vitro* experiments, where PsbO with reduced disulfide bond was incubated with proteases, revealed several degradation products. Band with lower molecular weight detected in our work most likely corresponds to F1 degradation product with molecular weight 32 kDa reported in Roberts et al. (2012). Our results imply that partially degraded PsbO is accumulated in lumen. This observation makes sense in case of HL treated plants. Finding of partially degraded PsbO in DA plants is more puzzling, one explanation may be economical. Plant preferentially invests energy in places of higher need. At night energy is mainly needed in stroma, where starch is enzymatically degraded. Therefore, plant waits with degradation of PsbO until the light period when there is excess energy in chloroplast for such a process.

Some blots incubated with anti-PsbO2 antibody exhibited nonspecific band approximately corresponding to molecular weight of 50 kDa. This band was visible also on blot with lumen in all HL treated samples. Since nonspecific band was also observed in *psbo2* mutant (Fig. 11), the possibility that it was conjugated PsbO2 can be excluded. According to literature, it may be a large subunit of RuBisCO enzyme (RBCL, 55 kDa). RBCL is bound to thylakoid membrane on the stroma side and it cannot be completely removed even by several wash steps (Kieselbach et al., 1998; Hall et al., 2010a). With regard to the absence of washing steps in my protocol, the band is most likely the result of nonspecific interaction caused by abundancy of RBLC.

6 Conclusions

- Mutant *psbo2* does not differ from wt in photosystem II subpopulations, amount of thylakoid subcompartments or soluble saccharide content.
- Absence of PsbO1 isoform fundamentally affects saccharide metabolism in *psbo1* mutant.
- PsbO isoforms are distributed heterogeneously in thylakoid membrane subcompartments. Both isoforms have highest levels in grana core and lowest levels in grana margins.
- Isoforms have different reaction in response to short light stress. PsbO2 significantly decreases in grana core after light stress. PsbO2 level increases in grana margins relative to grana core level.
- Both isoforms accumulate in high amounts in thylakoid lumen in response to light stress.

7 References

Abramowicz, D.A. and Dismukes, G.C. (1984). Manganese proteins isolated from spinach thylakoid membranes and their role in O2 evolution. I. A 56 kilodalton manganese-containing protein, a probable component of the coupling factor enzyme. BBA - Bioenerg. **765**: 309–317.

Adamska, I., Kloppstech, K., and Ohad, I. (1993). Early light-inducible protein in pea is stable during light stress but is degraded during recovery at low light intensity. J. Biol. Chem. **268**: 5438–44.

Albertsson, P.-Å. (2001). A quantitative model of the domain structure of the photosynthetic membrane. Trends Plant Sci. **6**: 349–354.

Alboresi, A., Caffarri, S., Nogue, F., Bassi, R., and Morosinotto, T. (2008). In silico and biochemical analysis of Physcomitrella patens photosynthetic antenna: Identification of subunits which evolved upon land adaptation. PLoS One **3**: e2033.

Allahverdiyeva, Y. et al. (2013). Arabidopsis plants lacking PsbQ and PsbR subunits of the oxygen-evolving complex show altered PSII super-complex organization and short-term adaptive mechanisms. Plant J. **75**: 671–684.

Allahverdiyeva, Y., Mamedov, F., Holmström, M., Nurmi, M., Lundin, B., Styring, S., Spetea, C., and Aro, E. (2009). Comparison of the electron transport properties of the psbo1 and psbo2 mutants of Arabidopsis thaliana. BBA - Bioenerg. **1787**: 1230–1237.

Allen, J.F., Bennett, J., Steinback, K.E., and Arntzen, C.J. (1981). Chloroplast protein phosphorylation couples plastoquinone redox state to distribution of excitation energy between photosystems. Nature **291**: 25–29.

Allen, J.F. and Forsberg, J. (2001). Molecular recognition in thylakoid structure and function. Trends Plant Sci. **6**: 317–326.

Andersson, B. and Anderson, J.M. (1980). Lateral heterogeneity in the distribution of chlorophyll-protein complexes of the thylakoid membranes of spinach chloroplasts. BBA - Bioenerg. **593**: 427–440.

Armbruster, U. et al. (2013). Arabidopsis CURVATURE THYLAKOID1 Proteins Modify Thylakoid Architecture by Inducing Membrane Curvature. Plant Cell **25**: 2661–2678.

Aro, E.-M., Virgin, I., and Andersson, B. (1993). Photoinhibition of Photosystem II. Inactivation, protein damage and turnover. Biochim. Biophys. Acta - Bioenerg. **1143**: 113–134.

Barber, J. (2012). Photosystem II: the water-splitting enzyme of photosynthesis. Cold Spring Harb. Symp. Quant. Biol. **77**: 295–307.

Ben-Shem, A., Frolow, F., and Nelson, N. (2003). Crystal structure of plant photosystem I. Nature **426**: 630–5.

Boekema, E.J., van Breemen, J.F., van Roon, H., and Dekker, J.P. (2000). Arrangement of photosystem II supercomplexes in crystalline macrodomains within the thylakoid membrane of green plant chloroplasts. J. Mol. Biol. **301**: 1123–33.

Bonardi, V., Pesaresi, P., Becker, T., Schleiff, E., Wagner, R., Pfannschmidt, T., Jahns, P., and Leister, D. (2005). Photosystem II core phosphorylation and photosynthetic acclimation require

two different protein kinases. Nature **437**: 1179–82.

Bricker, T.M. (1992). Oxygen evolution in the absence of the 33-kilodalton manganese-stabilizing protein. Biochemistry **31**: 4623–8.

Bricker, T.M. and Frankel, L.K. (2011). Auxiliary functions of the PsbO, PsbP and PsbQ proteins of higher plant Photosystem II: A critical analysis. J. Photochem. Photobiol. B Biol. **104**: 165–178.

Bricker, T.M., Roose, J.L., Fagerlund, R.D., Frankel, L.K., and Eaton-rye, J.J. (2012). The extrinsic proteins of Photosystem II ☆. BBA - Bioenerg. **1817**: 121–142.

Burnap, R.L. and Sherman, L.A. (1991). Deletion mutagenesis in Synechocystis sp. PCC6803 indicates that the Mn-stabilizing protein of photosystem II is not essential for O2 evolution. Biochemistry **30**: 440–6.

Cruz, J.A., Sacksteder, C.A., Kanazawa, A., and Kramer, D.M. (2001). Contribution of electric field (Delta psi) to steady-state transthylakoid proton motive force (pmf) in vitro and in vivo. control of pmf parsing into Delta psi and Delta pH by ionic strength. Biochemistry **40**: 1226–37.

Cuello, J. and Quiles, M.J. (2004). Fractionation of Thylakoid Membranes Into Grana and Stroma Thylakoids. Photosynth. Res. **274**: 1–9.

Dekker, J.P. and Boekema, E.J. (2005). Supramolecular organization of thylakoid membrane proteins in green plants. Biochim. Biophys. Acta **1706**: 12–39.

Duchoslav, M. and Fischer, L. (2015). Parallel subfunctionalisation of PsbO protein isoforms in angiosperms revealed by phylogenetic analysis and mapping of sequence variability onto protein structure. BMC Plant Biol. **15**: 133.

Dwyer, S.A., Chow, W.S., Yamori, W., Evans, J.R., Kaines, S., Badger, M.R., and von Caemmerer, S. (2012). Antisense reductions in the PsbO protein of photosystem II leads to decreased quantum yield but similar maximal photosynthetic rates. J. Exp. Bot. **63**: 4781–4795.

Enami, I., Yoshihara, S., Tohri, A., Okumura, A., Ohta, H., and Shen, J.-R. (2000). Cross-Reconstitution of Various Extrinsic Proteins and Photosystem II Complexes from Cyanobacteria, Red Algae and Higher Plants. Plant Cell Physiol **41**: 1354–1364.

Ettinger, W.F. and Theg, S.M. (1991). Physiologically Active Chloroplasts Contain Pools of Unassembled Extrinsic Proteins of the Photosynthetic Oxygen-evolving Enzyme Complex in the Thylakoid Lumen. J. Cell Biol. **115**: 321–328.

Ferreira, K.N. (2004). Architecture of the Photosynthetic Oxygen-Evolving Center. Science (80-.). **303**: 1831–1838.

Fork, D.C. and Satoh, K. (1986). The Control by State Transitions of the Distribution of Excitation Energy in Photosynthesis. Annu. Rev. Plant Physiol. **37**: 335–361.

Fristedt, R., Herdean, A., Blaby-Haas, C.E., Mamedov, F., Merchant, S.S., Last, R.L., and Lundin, B. (2015). PHOTOSYSTEM II PROTEIN33, a protein conserved in the plastid lineage, is associated with the chloroplast thylakoid membrane and provides stability to photosystem II supercomplexes in Arabidopsis. Plant Physiol. **167**: 481–92.

Fristedt, R., Willig, A., Granath, P., Crevecoeur, M., Rochaix, J.-D., and Vener, A. V. (2009). Phosphorylation of Photosystem II Controls Functional Macroscopic Folding of Photosynthetic Membranes in Arabidopsis. Plant Cell **21**: 3950–3964.

García-Cerdán, J.G., Kovács, L., Tóth, T., Kereïche, S., Aseeva, E., Boekema, E.J., Mamedov, F., Funk, C., and Schröder, W.P. (2011). The PsbW protein stabilizes the supramolecular organization of photosystem II in higher plants. Plant J. **65**: 368–81.

Goodchild, D.J., Björkman, O., Pyliotis, N.A. (1972). Chloroplast ultrastructure, leaf anatomy,

and content of chlorophyll and soluble protein in rainforest species. Carnegie Inst. Wash. **Year Book** : 102–107.

Goral, T.K., Johnson, M.P., Duffy, C.D.P., Brain, A.P.R., Ruban, A. V, and Mullineaux, C.W. (2012). Light-harvesting antenna composition controls the macrostructure and dynamics of thylakoid membranes in Arabidopsis.: 289–301.

Hall, M., Mata-Cabana, A., Akerlund, H.-E., Florencio, F.J., Schröder, W.P., Lindahl, M., and Kieselbach, T. (2010a). Thioredoxin targets of the plant chloroplast lumen and their implications for plastid function. Proteomics **10**: 987–1001.

Hall, M., Mata-Cabana, A., Åkerlund, H.E., Florencio, F.J., Schröder, W.P., Lindahl, M., and Kieselbach, T. (2010b). Thioredoxin targets of the plant chloroplast lumen and their implications for plastid function. Proteomics **10**: 987–1001.

Heddad, M. and Adamska, I. (2000). Light stress-regulated two-helix proteins in Arabidopsis thaliana related to the chlorophyll a/b-binding gene family. Proc. Natl. Acad. Sci. **97**: 3741–3746.

Herbstová, M., Tietz, S., Kinzel, C., Turkina, M. V, and Kirchhoff, H. (2012). Architectural switch in plant photosynthetic membranes induced by light stress.

Hohmann-Marriott, M.F. and Blankenship, R.E. (2011). Evolution of Photosynthesis. Annu. Rev. Plant Biol **62**: 515–48.

Hundal, T., Virgin, I., Styring, S., and Andersson, B. (1990). Changes in the organization of Photosystem II following light-induced D1-protein degradation. BBA - Bioenerg. **1017**: 235–241.

Ido, K., Nield, J., Fukao, Y., Nishimura, T., Sato, F., and Ifuku, K. (2014). Cross-linking Evidence for Multiple Interactions of the PsbP and PsbQ Proteins in a Higher Plant Photosystem II Supercomplex. J. Biol. Chem. **289**: 20150–20157.

Ifuku, K., Yamamoto, Y., Ono, T.-A., Ishihara, S., and Sato, F. (2005). PsbP protein, but not PsbQ protein, is essential for the regulation and stabilization of photosystem II in higher plants. Plant Physiol. **139**: 1175–84.

Jansson, S. (1999). A guide to the Lhc genes and their relatives in Arabidopsis. Trends Plant Sci. **4**: 236–240.

Jansson, S., Andersson, J., Kim, S.J., and Jackowski, G. (2000). An Arabidopsis thaliana protein homologous to cyanobacterial high-light-inducible proteins. Plant Mol. Biol. **42**: 345–51.

Järvi, S., Gollan, P.J., and Aro, E.-M. (2013). Understanding the roles of the thylakoid lumen in photosynthesis regulation. Front. Plant Sci. **4**: 434.

Järvi, S., Suorsa, M., and Aro, E.-M. (2015). Photosystem II repair in plant chloroplasts — Regulation, assisting proteins and shared components with photosystem II biogenesis. Biochim. Biophys. Acta - Bioenerg. **1847**: 900–909.

Joliot, P. (2003). Period-four oscillations of the flash-induced oxygen formation in photosynthesis. Photosynth. Res. **76**: 65–72.

Junge, W., Sielaff, H., and Engelbrecht, S. (2009). Torque generation and elastic power transmission in the rotary F(O)F(1)-ATPase. Nature **459**: 364–70.

Khatoon, M., Inagawa, K., Pospísil, P., Yamashita, A., Yoshioka, M., Lundin, B., Horie, J., Morita, N., Jajoo, A., Yamamoto, Y., and Yamamoto, Y. (2009). Quality control of photosystem II: Thylakoid unstacking is necessary to avoid further damage to the D1 protein and to facilitate D1 degradation under light stress in spinach thylakoids. J. Biol. Chem. **284**: 25343–52.

Kieselbach, T., Hagman, Å., Andersson, B., and Schro, W.P. (1998). The Thylakoid Lumen of Chloroplasts. **273**: 6710–6716.

Kirchhoff, H. (2013a). Architectural switches in plant thylakoid membranes. Photosynth. Res. **116**: 481–487.

Kirchhoff, H. (2014). Structural changes of the thylakoid membrane network induced by high light stress in plant chloroplasts. Philos. Trans. R. Soc. Lond. B. Biol. Sci. **369**: 20130225.

Kirchhoff, H. (2013b). Structural constraints for protein repair in plant photosynthetic membranes. Plant Signal. Behav. **8**: e23634.

Kirchhoff, H., Haferkamp, S., Allen, J.F., Epstein, D.B.A., and Mullineaux, C.W. (2008). Protein diffusion and macromolecular crowding in thylakoid membranes. Plant Physiol. **146**: 1571–8.

Kirchhoff, H., Hall, C., Wood, M., Herbstova, M., Tsabari, O., Nevo, R., Charuvi, D., Shimoni, E., and Reich, Z. (2011). Dynamic control of protein diffusion within the granal thylakoid lumen. Proc. Natl. Acad. Sci. **108**: 20248–20253.

Klimmek, F., Sjödin, A., Noutsos, C., Leister, D., and Jansson, S. (2006). Abundantly and rarely expressed Lhc protein genes exhibit distinct regulation patterns in plants. Plant Physiol. **140**: 793–804.

Kok, B., Forbush, B., and McGloin, M. (1970). Cooperation of charges in photosynthetic O2 evolution-I. A linear four step mechanism. Photochem. Photobiol. **11**: 457–75.

Komenda, J. and Barber, J. (1995). Comparison of psbO and psbH deletion mutants of Synechocystis PCC 6803 indicates that degradation of D1 protein is regulated by the QB site and dependent on protein synthesis. Biochemistry **34**: 9625–31.

Kouřil, R., Dekker, J.P., and Boekema, E.J. (2012). Supramolecular organization of photosystem II in green plants. Biochim. Biophys. Acta **1817**: 2–12.

Kouřil, R., Oostergetel, G.T., and Boekema, E.J. (2011). Fine structure of granal thylakoid membrane organization using cryo electron tomography. Biochim. Biophys. Acta - Bioenerg. **1807**: 368–374.

Kramer, D.M., Sacksteder, C.A., and Cruz, J.A. (1999). How acidic is the lumen ?: 151–163.

Kyle, D.J., Ohad, I., and Arntzen, C.J. (1984). Membrane protein damage and repair: Selective loss of a quinone-protein function in chloroplast membranes. Proc. Natl. Acad. Sci. U. S. A. **81**: 4070–4.

De Las Rivas, J., Balsera, M., and Barber, J. (2004). Evolution of oxygenic photosynthesis: genome-wide analysis of the OEC extrinsic proteins. Trends Plant Sci. **9**: 18–25.

De Las Rivas, J. and Barber, J. (2004). Analysis of the structure of the PsbO protein and its implications. Photosynth. Res. **81**: 329–343.

De Las Rivas, J. and Roman, A. (2005). Structure and evolution of the extrinsic proteins that stabilize the oxygen-evolving engine. Photochem. Photobiol. Sci. **4**: 1003–1010.

Li, X.P., Björkman, O., Shih, C., Grossman, A.R., Rosenquist, M., Jansson, S., and Niyogi, K.K. (2000). A pigment-binding protein essential for regulation of photosynthetic light harvesting. Nature **403**: 391–5.

Lipavska, H., Svobodova, H., Albrechtova, J., Kumstyrova, L., Vagner, M., and Vondrakova, Z. (2000). Carbohydrate status during somatic embryo maturation in Norway spruce. Vitr. Cell. Dev. Biol. **36**: 260–267.

Lipavska, H. and Vreugdenhil, D. (1996). Uptake of mannitol from the media by in vitro grown plants. Plant Cell. Tissue Organ Cult. **45**: 103–107.

Liu, Z., Yan, H., Wang, K., Kuang, T., Zhang, J., Gui, L., An, X., and Chang, W. (2004). Crystal structure of spinach major light-harvesting complex at 2.72 A resolution. Nature **428**: 287–92.

Ljungberg, U., Åkerlung, H.-E., Larsson, C., and Andersson, B. (1984). Identification of polypeptides associated with the 23 and 33 kDa proteins of photosynthetic oxygen evolution. Biochim. Biophys. Acta - Bioenerg. **767**: 145–152.

Lu, Y.K., Theg, S.M., and Stemler, A.J. (2005). Carbonic anhydrase activity of the photosystem II OEC33 protein from pea. Plant Cell Physiol. **46**: 1944–1953.

Lundin, B., Hansson, M., Schoefs, B., Vener, A. V, and Spetea, C. (2007a). The Arabidopsis PsbO2 protein regulates dephosphorylation and turnover of the photosystem II reaction centre D1 protein. Plant J. **49**: 528–539.

Lundin, B., Nurmi, M., Rojas-Stuetz, M., Aro, E.-M., Adamska, I., and Spetea, C. (2008). Towards understanding the functional difference between the two PsbO isoforms in Arabidopsis thaliana—insights from phenotypic analyses of psbo knockout mutants. Photosynth. Res. **98**: 405–414.

Lundin, B., Thuswaldner, S., Shutova, T., Eshaghi, S., Samuelsson, G., Barber, J., Andersson, B., and Spetea, C. (2007b). Subsequent events to GTP binding by the plant PsbO protein: Structural changes, GTP hydrolysis and dissociation from the photosystem II complex. Biochim. Biophys. Acta - Bioenerg. **1767**: 500–508.

Lydakis-Simantiris, N., Hutchison, R.S., Betts, S.D., Barry, B.A., and Yocum, C.F. (1999). Manganese stabilizing protein of photosystem II is a thermostable, natively unfolded polypeptide. Biochemistry **38**: 404–14.

Mayes, S.R., Cook, K.M., Self, S.J., Zhang, Z., and Barber, J. (1991). Deletion of the gene encoding the Photosystem II 33 kDa protein from Synechocystis sp. PCC 6803 does not inactivate water-splitting but increases vulnerability to photoinhibition. Biochim. Biophys. Acta - Bioenerg. **1060**: 1–12.

Mayfield, S.P., Bennoun, P., and Rochaix, J.D. (1987). Expression of the nuclear encoded OEE1 protein is required for oxygen evolution and stability of photosystem II particles in Chlamydomonas reinhardtii. EMBO J. **6**: 313–8.

McFadden, G.I. and Van Dooren, G.G. (2004). Evolution: Red algal genome affirms a common origin of all plastids. Curr. Biol. **14**: R514–R516.

Melis, A. (1999). Photosystem-II damage and repair cycle in chloroplasts: what modulates the rate of photodamage in vivo? Trends Plant Sci. **4**: 130–135.

Mellis, A. (1999). Photosystem-II damage and repair cycle in chloroplasts: What modulates the rate of photodamage in vivo? Trends Plant Sci. **4**: 130–135.

Meyer, Y., Buchanan, B.B., Vignols, F., and Reichheld, J.-P. (2009). Thioredoxins and Glutaredoxins: Unifying Elements in Redox Biology. http://dx.doi.org/10.1146/annurev-genet-102108-134201.

Miyao, M. and Murata, N. (1984). Role of the 33-kDa polypeptide in preserving Mn in the photosynthetic oxygen-evolution system and its replacement by chloride ions. FEBS Lett. **170**: 350–354.

Mullineaux, C.W. (2005). Function and evolution of grana. Trends Plant Sci. **10**: 521–525.

Mulo, P., Sirpiö, S., Suorsa, M., and Aro, E.M. (2008). Auxiliary proteins involved in the assembly and sustenance of photosystem II. Photosynth. Res. **98**: 489–501.

Murakami, R., Ifuku, K., Takabayashi, A., Shikanai, T., Endo, T., and Sato, F. (2002). Characterization of an Arabidopsis thaliana mutant with impaired psb O, one of two genes encoding extrinsic 33-kDa proteins in photosystem II. FEBS Lett. **523**: 138–142.

Murakami, R., Ifuku, K., Takabayashi, A., Shikanai, T., Endo, T., and Sato, F. (2005). Functional dissection of two Arabidopsis PsbO proteins. FEBS J. **272**: 2165–2175.

Mustárdy, L. and Garab, G. (2003). Granum revisited. A three-dimensional model – where things fall into place. Trends Plant Sci. **8**: 117–122.

Neidhardt, J., Benemann, J.R., Zhang, L., and Melis, A. (1998). Photosystem-II repair and chloroplast recovery from irradiance stress: relationship between chronic photoinhibition, light-harvesting chlorophyll antenna size and photosynthetic productivity in Dunaliella salina (green algae). Photosynth. Res. **56**: 175–184.

Nickelsen, J. and Rengstl, B. (2013). Photosystem II assembly: from cyanobacteria to plants. Annu. Rev. Plant Biol. **64**: 609–35.

Nield, J. and Barber, J. (2006). Refinement of the structural model for the Photosystem II supercomplex of higher plants. Biochim. Biophys. Acta - Bioenerg. **1757**: 353–361.

Nixon, P.J., Michoux, F., Yu, J., Boehm, M., and Komenda, J. (2010). Recent advances in understanding the assembly and repair of photosystem II. Ann. Bot. **106**: 1–16.

Niyogi, K.K. (1999). PHOTOPROTECTION REVISITED: Genetic and Molecular Approaches. Annu. Rev. Plant Physiol. Plant Mol. Biol. **50**: 333–359.

Ohad, I., Kyle, D.J., and Arntzen, C.J. (1984). Membrane protein damage and repair: removal and replacement of inactivated 32-kilodalton polypeptides in chloroplast membranes. J. Cell Biol. **99**: 481–5.

Peltier, J.-B., Emanuelsson, O., Kalume, D.E., Ytterberg, J., Friso, G., Rudella, A., Liberles, D.A., Söderberg, L., Roepstorff, P., von Heijne, G., and van Wijk, K.J. (2002). Central functions of the lumenal and peripheral thylakoid proteome of Arabidopsis determined by experimentation and genome-wide prediction. Plant Cell **14**: 211–36.

Philbrick, J.B., Diner, B.A., and Zilinskas, B.A. (1991). Construction and characterization of cyanobacterial mutants lacking the manganese-stabilizing polypeptide of photosystem II. J. Biol. Chem. **266**: 13370–6.

Popelkova, H., Im, M.M., D'Auria, J., Betts, S.D., Lydakis-Simantiris, N., and Yocum, C.F. (2002). N-Terminus of the Photosystem II Manganese Stabilizing Protein: Effects of Sequence Elongation and Truncation †. Biochemistry **41**: 2702–2711.

Popelkova, H. and Yocum, C.F. (2011). PsbO, the manganese-stabilizing protein: Analysis of the structure-function relations that provide insights into its role in photosystem II. J. Photochem. Photobiol. B Biol. **104**: 179–190.

Porra, R.J., Thompson, W.A., and Kriedemann, P.E. (1989). Determination of accurate extinction coefficients and simultaneous equations for assaying chlorophylls a and b extracted with four different solvents: verification of the concentration of chlorophyll standards by atomic absorption spectroscopy. Biochim. Biophys. Acta - Bioenerg. **975**: 384–394.

Pribil, M., Labs, M., and Leister, D. (2014). Structure and dynamics of thylakoids in land plants. **65**: 1955–1972.

Puthiyaveetil, S., Tsabari, O., Lowry, T., Lenhert, S., Lewis, R.R., Reich, Z., and Kirchhoff, H. (2014). Compartmentalization of the protein repair machinery in photosynthetic membranes. Proc. Natl. Acad. Sci. **111**: 15839–15844.

Rast, A., Heinz, S., and Nickelsen, J. (2015). Biogenesis of thylakoid membranes. BBA - Bioenerg.: 1–10.

Roberts, I.N., Lam, X.T., Miranda, H., Kieselbach, T., and Funk, C. (2012). Degradation of PsbO by the Deg Protease HhoA Is Thioredoxin Dependent. PLoS One **7**: e45713.

Rolland, F., Baena-Gonzalez, E., and Sheen, J. (2006). Sugar Sensing and Signaling in Plants: Conserved and Novel Mechanisms. Annu. Rev. Plant Biol **57**: 675–709.

Roose, J.L., Frankel, L.K., Mummadisetti, M.P., and Bricker, T.M. (2016). The extrinsic proteins of photosystem II: update. Planta **243**: 889–908.

Samol, I., Shapiguzov, A., Ingelsson, B., Fucile, G., Crèvecoeur, M., Vener, A. V, Rochaix, J.-D., and Goldschmidt-Clermont, M. (2012). Identification of a photosystem II phosphatase involved in light acclimation in Arabidopsis. Plant Cell **24**: 2596–609.

Schubert, M., Petersson, U.A., Haas, B.J., Funk, C., Schroder, W.P., and Kieselbach, T. (2002). Proteome Map of the Chloroplast Lumen of Arabidopsis thaliana. J. Biol. Chem. **277**: 8354–8365.

Shi, L.-X. and Schröder, W.P. (2004). The low molecular mass subunits of the photosynthetic supracomplex, photosystem II. Biochim. Biophys. Acta - Bioenerg. **1608**: 75–96.

Shinozaki, K. et al. (1986). The complete nucleotide sequence of the tobacco chloroplast genome: its gene organization and expression. EMBO J. **5**: 2043–2049.

Shutova, T., Nikitina, J., Deikus, G., Andersson, B., Klimov, V., and Samuelsson, G. (2005). Structural dynamics of the manganese-stabilizing protein-effect of pH, calcium, and manganese. Biochemistry **44**: 15182–15192.

Spetea, C., Hundal, T., Lohmann, F., and Andersson, B. (1999). GTP bound to chloroplast thylakoid membranes is required for light-induced, multienzyme degradation of the photosystem II D1 protein. Proc. Natl. Acad. Sci. U. S. A. **96**: 6547–52.

Spetea, C., Hundal, T., Lundin, B., Heddad, M., Adamska, I., and Andersson, B. (2004). Multiple evidence for nucleotide metabolism in the chloroplast thylakoid lumen. Proc. Natl. Acad. Sci. U. S. A. **101**: 1409–1414.

Standfuss, J. and Kühlbrandt, W. (2004). The three isoforms of the light-harvesting complex II: spectroscopic features, trimer formation, and functional roles. J. Biol. Chem. **279**: 36884–91.

Stettler, M., Eicke, S., Mettler, T., Messerli, G., H??rtensteiner, S., and Zeeman, S.C. (2009). Blocking the metabolism of starch breakdown products in arabidopsis leaves triggers chloroplast degradation. Mol. Plant **2**: 1233–1246.

Strittmatter, P., Soll, J., and Bölter, B. (2010). The chloroplast protein import machinery: a review. Methods Mol. Biol. **619**: 307–21.

Suorsa, M. and Aro, E.M. (2007). Expression, assembly and auxiliary functions of photosystem II oxygen-evolving proteins in higher plants. Photosynth. Res. **93**: 89–100.

Suorsa, M., Rantala, M., Danielsson, R., Järvi, S., Paakkarinen, V., Schröder, W.P., Styring, S., Mamedov, F., and Aro, E.-M. (2014). Dark-adapted spinach thylakoid protein heterogeneity offers insights into the photosystem II repair cycle. Biochim. Biophys. Acta - Bioenerg. **1837**: 1463–1471.

Suorsa, M., Rossi, F., Tadini, L., Labs, M., Colombo, M., Jahns, P., Kater, M.M., Leister, D., Finazzi, G., Aro, E.-M., Barbato, R., and Pesaresi, P. (2016). PGR5-PGRL1-Dependent Cyclic Electron Transport Modulates Linear Electron Transport Rate in Arabidopsis thaliana. Mol. Plant **9**: 271–288.

Tikhonov, A.N. (2013). pH-dependent regulation of electron transport and ATP synthesis in chloroplasts. Photosynth. Res. **116**: 511–34.

Tikkanen, M., Nurmi, M., Kangasjärvi, S., and Aro, E.-M. (2008). Core protein phosphorylation facilitates the repair of photodamaged photosystem II at high light. Biochim. Biophys. Acta - Bioenerg. **1777**: 1432–1437.

Umena, Y., Kawakami, K., Shen, J., and Kamiya, N. (2011). Crystal structure of oxygen-evolving photosystem II at a resolution of 1.9 Å. Nature **473**: 55–60.

Uversky, V.N., Gillespie, J.R., and Fink, A.L. (2000). Why are "natively unfolded" proteins unstructured under physiologic conditions? Proteins **41**: 415–27.

Vinyard, D.J., Ananyev, G.M., and Charles Dismukes, G. (2013). Photosystem II: The Reaction Center of Oxygenic Photosynthesis*. Annu. Rev. Biochem. **82**: 577–606.

Wei, X., Su, X., Cao, P., Liu, X., Chang, W., Li, M., Zhang, X., and Liu, Z. (2016). Structure of spinach photosystem II–LHCII supercomplex at 3.2 Å resolution. Nature **534**: 69–74.

Wollenberger, L., Weibull, C., and Albertsson, P.-Å. (1995). Further characterization of the chloroplast grana margins: the non-detergent preparation of granal Photosystem I cannot reduce ferredoxin in the absence of NADP+ reduction. Biochim. Biophys. Acta - Bioenerg. **1230**: 10–22.

Wyman, A.J. and Yocum, C.F. (2005). Assembly and function of the photosystem II manganese stabilizing protein: lessons from its natively unfolded behavior. Photosynth. Res. **84**: 283–8.

Yi, X., Hargett, S.R., Frankel, L.K., and Bricker, T.M. (2009). The PsbP protein, but not the PsbQ protein, is required for normal thylakoid architecture in Arabidopsis thaliana. FEBS Lett. **583**: 2142–2147.

Yi, X., Hargett, S.R., Frankel, L.K., and Bricker, T.M. (2006). The PsbQ protein is required in Arabidopsis for photosystem II assembly/stability and photoautotrophy under low light conditions. J. Biol. Chem. **281**: 26260–7.